Electronic Supplementary Information (ESI)

Ruthenium catalyzed transformation of levulinic acid to γ-valerolactone in water

Bhanu Priya,[†] Vinod K. Sahu[†] and Sanjay K. Singh[*]

Catalysis group, Department of Chemistry, Indian Institute of Technology Indore, Simrol, Indore 453552, India.

E-mail: sksingh@iiti.ac.in

[†] Equal contribution

General Information, Materials, and Instrumentation. All reactions were performed using high purity chemicals purchased from Sigma Aldrich, TCI chemicals and Alfa Aesar. Chemicals purchased were used as received without any further purification. The ^{1}H NMR (400 MHz and 500 MHz), ^{13}C NMR (100 MHz and 125 MHz) and ^{31}P NMR (162 MHz and 202 MHz) spectra are recorded at 298 K using DMSO-d_6 methanol-d_4, or $CDCl_3$ as the solvent on a Bruker Advance 400 and Bruker Ascend 500 spectrometer. Tetramethylsilane (TMS) is used as an external standard and the chemical shifts in ppm are reported relative to the centre of the singlet at 3.35 and 4.78 for methanol-d_4, 2.49 ppm for DMSO-d_6 and 7.26 for $CDCl_3$ in ^{1}H NMR and to 49.3 ppm for methanol-d_4, 39.50 ppm for DMSO-d_6 and 77.0 for $CDCl_3$ in ^{13}C NMR. ESI (positive mode), and liquid chromatography mass spectroscopy (LCMS) are recorded on a micro-TF-Q II mass spectrometer. Single crystal was obtained by diffusion of diethyl ether into methanolic solution of the complex. Suitable single crystals of complexes **[Ru]-4, [Ru]-5 and [Ru]-8** were subjected to single-crystal X-ray structural studies using CCD Agilent Technologies (Oxford Diffraction) Super NOVA diffractometer. Data are collected at 150(2) K using graphite-monochromated Mo Kα radiation (λα = 0.71073 A). The strategy for the data collection

evaluated using the CrysAlisPro CCD software. The crystal and refinement data are summarized in Table 1 (in manuscript). Selected bond lengths and bond angles are summarized in Tables S1 and S2. CCDC deposition numbers of the complexes **[Ru]-4**, **[Ru]-5** and **[Ru]-8** are 1971292, 1971295 and 1971294 respectively. ICP-AES data was recorded using ARCOS, Simultaneous ICP Spectrometer, SPECTRO Analytical Instruments GmbH, Germany.

Table S1. Comparative chart showing literature available Ru-based catalytic systems for transformation of LA to GVL.

Catalytic system	**Solvent**	**Additive**	**H_2 source**	**T(°C)/ t(h)**	**TON**	**TOF (h^{-1})**	**Conv. (%) of LA**	**Sel./Yield (%) of GVL**	**Ref.**
$Ru(acac)_3$/TPPTS	water	-	70 bar H_2	140/12	600	50	>99.9	100/95	S1
$RuCl_3/PPh_3$	water	pyridine	HCOOH	150/6	930	155	>99.9	100/93	S2
$Ru(acac)_3$/PPMDP	neat	*p*-TsOH	80 bar H_2	140/168	75855	452	n.d.	n.d./76	S3
$Ru(acac)_3$/Bu-DPPDS	neat	-	100 bar H_2	140/1.8	6370	3540	>99.9	100/>99	S4
$[RuH_2(CO)$ (Triphos)]	neat	-	100 bar H_2	160/18	1000	56	>99.9	90/90	S5
Shvo catalyst	neat	-	HCOOH	95/6	1065	177	>99.9	>99/>99	S6
[Ru(*p*-cymene)Cl (DPDP)][BArF]	neat	KOH	HCOOH	120/16	960	60	96	100/n.d.	S7
[Ru(*p*-cymene)Cl (QMABA)]	neat	KOH, Et_3N	HCOOH	150/12	980	81.6	98	100/n.d.	S8
$[Ru(CO_3)(CO)$ (Triphos)]	1,4-dioxane	-	50 bar H_2	130/25	1200	48	>99	60/60	S9
$[\{Ru(p\text{-cymene})Cl\}_2$ TEPMP][$2BPh_4$]	neat	Et_3N	HCOOH	120/8	990	123	100	97/n.d.	S10
[{η^4-2,3,4,5-$Ph_4(C_4CO)$} $Ru(CO)_3$]	neat	-	50 bar H_2	100/5	720	144	100	100/99.1	S11
[η^6-*p*-cymene)RuCl (κ^2-pyNH^{n}pr)]$^+$	**water**	**Et_3N**	**HCOOH**	**80/2**	**40**	**20**	**>99.9**	**100/87[a]**	**This work**

TPPTS: triphenylphosphine trisulfonate, Bu-DPPDS: dibutyl(phenylphosphine)(*m*-disulphonate), PPMDP: {[(phenylphosphinediyl)bis-(1,2-phenylene)]bis(methylene)}bis-(diphenylphosphine), BArF: tetrakis[3,5-bis(trifluoromethyl)phenyl]borate, DPDP: 1-[2-{(diphenylphosphaneyl)oxy}ethyl]-3,5-dimethyl-1H-pyrazole, QMABA: 4-[(quinolin-2-ylmethylene)amino] benzoic acid, TEPMP: Tetraethyl ethane-1,2-diylbis((pyridin-2-ylmethyl)phosphoramidite),

[a]isolated yield, n.d. – not determined.

Table S2. Crystal Refinement data of complexes **[Ru]-4**, **[Ru]-5** and **[Ru]-8**.

crystal parameter	**complex [Ru]-4**	**complex [Ru]-5**	**complex [Ru]-8**
empirical formula	$C_{20}H_{30}ClF_6N_2PRu$	$C_{20}H_{30}ClF_6N_2PRu$	$C_{21}H_{32}ClF_6N_2PRu$
formula weight	579.95	579.95	593.97
temperature (K)	293	293	298
wavelength (Å)	1.54184	1.54184	1.54184
crystal system	triclinic	monoclinic	orthorhombic
space group	*P-1*	$P2_1/c$	*P*bca
crystal size (mm^3)	0.23 x 0.18 x 0.14	0.22 x 0.19 x 0.17	0.31 x 0.21 x 0.18
a (Å)	9.3898(7)	10.9086(2)	17.5759(4)
b (Å)	11.9327(9)	9.2051(2)	15.4169(2)
c (Å)	12.8169(7)	24.7878(4)	18.4534(4)
α (°)	100.642(6)	90	90.0(1)
β (°)	109.691(7)	99.912(2)	90.0(1)
γ (°)	107.961(7)	90	90.0(1)
V ($Å^3$)	1217.62(19)	2451.91(8)	5000.23(17)
Z	2	4	8
ρ (g/cm^3)	1.582	1.571	1.578
μ (mm^{-1})	7.354	7.304	7.178
F (000)	588	1176.0	2416.0
2θ range for data collection (°)	7.74 to 142.92	7.24 to 143.766	9.01 to 124.984
index ranges	$-11 \le h \le 10$, $-14 \le k \le 11$, $-14 \le l \le 15$	$-13 \le h \le 13$, $-11 \le k \le 11$, $-29 \le l \le 30$	$-19 \le h \le 20$, $-17 \le k \le 17$, $-21 \le l \le 16$
reflections collected/ independent reflections	8535/4635 [R_{int} = 0.0888]	15956/4708 [R_{int} = 0.1181]	32327/3980 [R_{int} = 0.1484]
data/restraints/parameters	4635/1/281	4708/0/285	3980/105/295
goodness-of-fit on F^2	1.132	1.263	1.088
final R indexes [$I > 2\sigma(I)$]	R_1 = 0.0667, wR_2 = 0.1520	R_1 = 0.1026, wR_2 = 0.2923	R_1 = 0.0680, wR_2 = 0.1904

R indexes (all data)	R_1 = 0.0776, wR_2 = 0.1636	R_1 = 0.1159, wR_2 = 0.3268	R_1 = 0.0827, wR_2 = 0.2126
Largest diff. peak/hole ($eÅ^{-3}$)	1.59/-1.22	1.80/-1.28	1.32/-1.16

Table S3. Important bond lengths (Å) for complex **[Ru]-4**, **[Ru]-5, [Ru]-8.**

	[Ru]-4	**[Ru]-5**	**[Ru]-8**
Ru-C_t	1.676	1.679	1.687
Ru-C_{avg}	2.183	2.195	2.200
Ru-N_{py}	2.099(6)	2.089(7)	2.079(5)
Ru-N_{amine}	2.127(5)	2.138(7)	2.196(7)
Ru-Cl	2.406(16)	2.398(2)	2.392(18)
N_{amine}-C_6	1.468(8)	1.442(13)	1.492(9)

Table S4. Important bond bond Angles (°) and torsion angles (°) for complex **[Ru]-4**, **[Ru]-5, [Ru]-8.**

Bond Angles (°)

	[Ru]-4	**[Ru]-5**	**[Ru]-8**
N_{py}-Ru-N_{amine}	78.1(2)	76.9(3)	76.1(2)
N_{py}-Ru-Cl	84.32(16)	83.89(19)	85.68(14)
N_{amine}-Ru-Cl	84.60(13)	82.8(2)	82.55(19)
N_{amine}-Ru-C_t	132.35	133.62	137.38
N_{py}-Ru-C_t	131.98	131.61	129.24
C_t-Ru-Cl	127.33	128.69	126.82
Torsion Angles (°)			
N_{py}-C_5-C_6-N_{amine}	-30.36(8)	-17.71	27.34

General procedure for the synthesis of pyridylamine (L2 – L8) ligands. *N*-pyridylamine ligands **L2 – L8** were synthesized by following the previously reported two step procedures.[S12-S16] Typically, in Step-I, condensation of pyridine-2-carboxaldehyde (1 equiv.) and corresponding

amine (1.0 ~ 10.0 equiv.) in THF (20 mL) at room temperature was carried out for 24 h. The progress of the reaction was monitored by TLC (thin layer chromatography). After reaction completion, all the volatiles were removed under reduced pressure and product obtained was analysed by ^{1}H NMR and then used in next step. In the next step, the compound obtained from previous step was dissolved in methanol (20 mL) followed by addition of 0.946 g $NaBH_4$ under ice-cold conditions. Then the reaction mixture was allowed to stir for 24 h at room temperature. Methanol was then removed under reduced pressure and the obtained crude product was extracted with dichloromethane and water to remove excess $NaBH_4$. Volatiles are removed under reduced pressure and analysed by ^{1}H and ^{13}C NMR and used without further purification.

Table S5. Effect of catalyst loading on catalytic transformation of LA to GVL.[a]

Entry	**Catalyst loading (mol%)**	**t (h)**	**Conv. (%)**	**GVL Sel./Yield[b] (%)**	**TOF (h^{-1})**
1	0.25	24	92	83/72	15
2	1.0	6	98	>99/94	16
3	2.5	2	>99	>99/95	20

[a]Reaction condition: **[Ru]-2** catalyst, LA (1 mmol), HCOOH (6 mmol), Et_3N (1 mmol), water (5 mL), 80 °C, 2 h. [b]Yield is calculated using maleic acid as an internal standard.

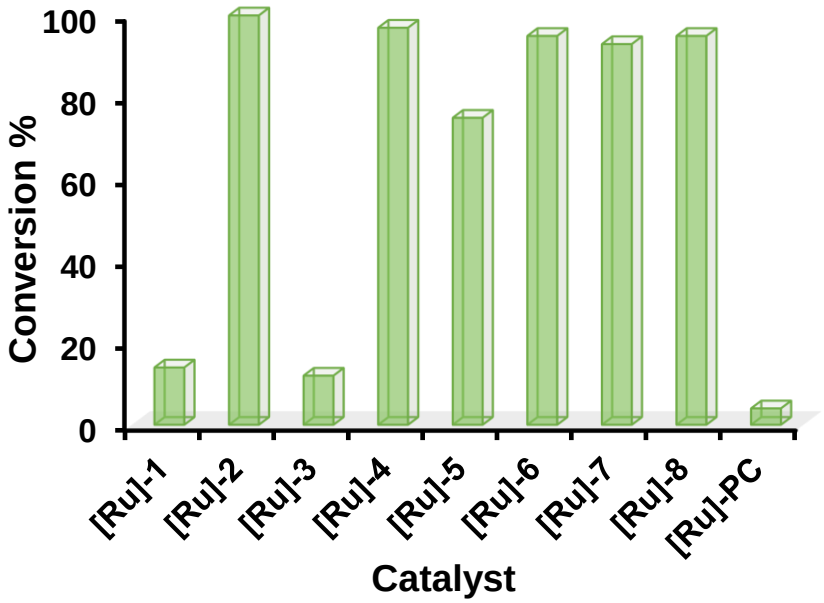

Fig. S1 Comparative catalytic activity of (η^6-*p*-cymene)Ru(II)-pyridylamine complexes (**[Ru]-1 – [Ru]-8**) for the transformation of LA to GVL. Reaction conditions: Ruthenium catalyst (2.5 mol%), LA (1 mmol), HCOOH (6 mmol), Et_3N (1 mmol), water (5 mL), 80 °C, 2h.

Table S6. Effect of temperature on catalytic transformation of LA to GVL.[a]

Entry	T (°C)	Conv. (%)	GVL Sel./Yield[b] (%)
2	70	10	72/6.5
3	80	18	66/11
4	90	26	77/19
5	100	40	83/31

[a]Reaction condition: **[Ru]-2** catalyst (2.5 mol%), LA (1 mmol), HCOOH (6 mmol), Et_3N (1 mmol), water (5 mL), 15 min, 70-100 °C. [b]Yield is calculated using maleic acid as an internal standard.

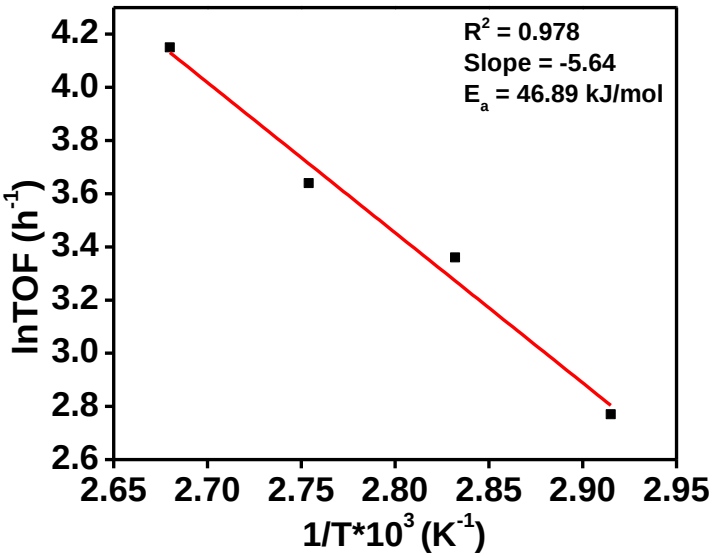

Fig. S2 Arrhenius plot for the catalytic transformation of LA to GVL over **[Ru]-2**. (Based on the data shown in Table S5)

Table S7. Effect of various bases on catalytic transformation of LA to GVL.[a]

Entry	Base	Conv. (%)	GVL Sel./Yield[b] (%)
1	HCOONa	94	97/86
2	NaOH	92	93/77
3	$NaHCO_3$	62	90/53
4	K_3PO_4	83	94/76
5	Et_3N	>99	>99/95
6[c]	-	8	98/5

[a]Reaction condition: **[Ru]-2** catalyst (2.5 mol%), LA (1 mmol), HCOOH (6 mmol), base (1 mmol), water (5 mL), 80 °C, 2 h. [b]Yield is calculated using maleic acid as an internal standard. [c]Reaction performed without base.

Table S8. Effect of reaction time on catalytic transformation of LA to GVL[a]

Entry	t (h)	Conv. (%)	Sel. (%)	
			4-HPA	GVL
1.	0.5	52	80	20
2.	1	80	70	30
3.	1.5	97	52	48
4.	2	>99	-	>99

[a]Reaction condition: **[Ru]-2** catalyst (2.5 mol%), LA (1 mmol), HCOOH (6 mmol), Et_3N (1 mmol), water (5 mL), 80 °C, 0.5-2 h.

Table S9. Effect of pH on catalytic transformation of LA to GVL.[a]

Entry	HCOOH (equiv.)	Et_3N (equiv.)	pH	Conv. (%)	Sel./Yield (%)	
					4-HPA	GVL
1	1	1	6.1	35	43/9	57/16
2	3	1	4.7	95	25/18	75/58
3	5	1	3.6	>99	16/11	84/72
4	6	1	2.7	>99	-	>99/85

[a]Reaction condition: **[Ru]-2** (2.5 mol%), LA (1 mmol), HCOOH (1-6 mmol), Et_3N (1 mmol), water (5 mL) 80 °C, 2 h.

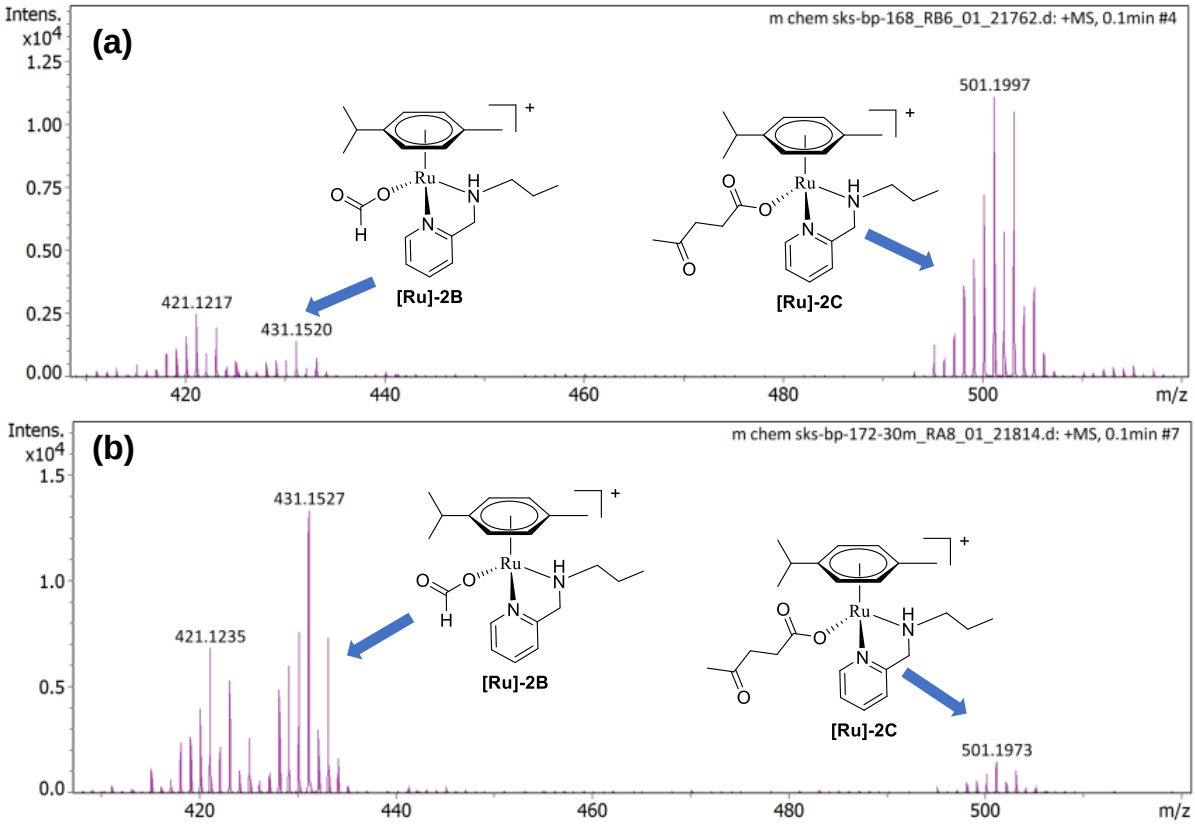

Fig. S3 Observed mass data for Ru-formato (**[Ru]-2B**) and Ru-levulinate (**[Ru]-2C**) species for (a) 3:1 and (b) 6:1 HCOOH:Et_3N after 1 h reaction time.

Table S10. Catalytic recyclability for the transformation of LA to GVL over **[Ru]-2** complex.[a]

Entry	Catalytic run	Conv. (%)	Sel. (%)/Yield (%)
1	1st	>99	99/85
2	2nd	>99	99/85
3	3rd	>99	99/84
4	4th	82	94/71
5	5th	74	81/53

[a]Reaction condition: **[Ru]-2** catalyst (2.5 mol%), LA (1 mmol), HCOOH (6 mmol), Et_3N (1 mmol), water (5 mL), 80 °C, 2 h.

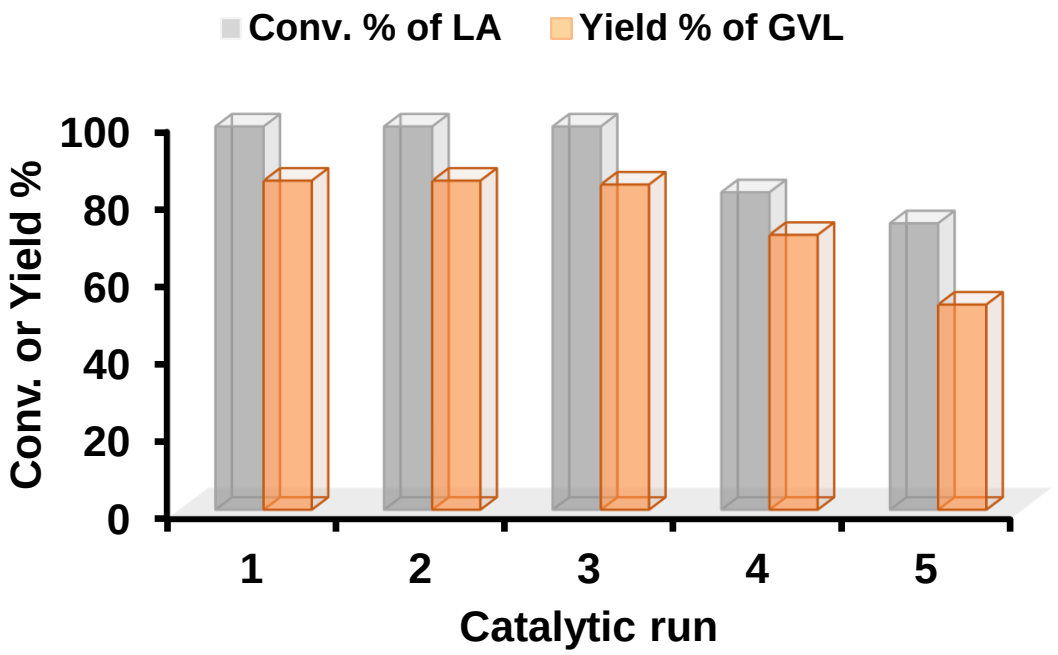

Fig. S4 Catalytic recyclability for transformation of LA to GVL over **[Ru]-2** complex. Reaction conditions: **[Ru]-2** (2.5 mol%), LA (1 mmol), HCOOH (6 mmol), Et_3N (1 mmol), water (5 mL).

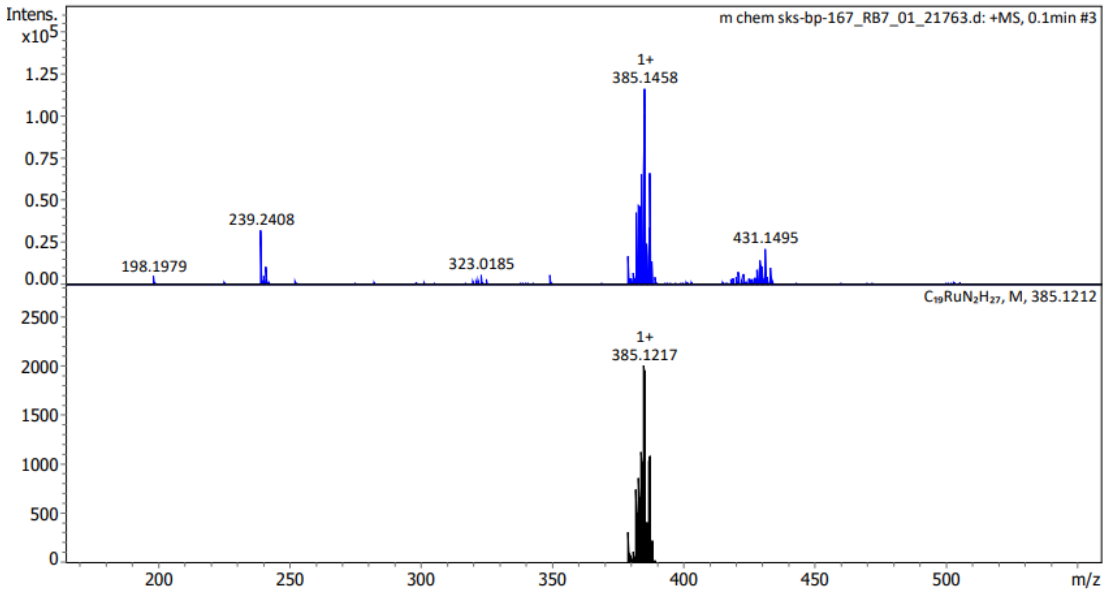

Fig. S5 Observed and simulated pattern for **[Ru]-2** catalyst after reaction.

Mass and NMR spectra of (η^6-p-cymene)Ru(II)-pyridylamine complexes [Ru]-1 – [Ru]-8

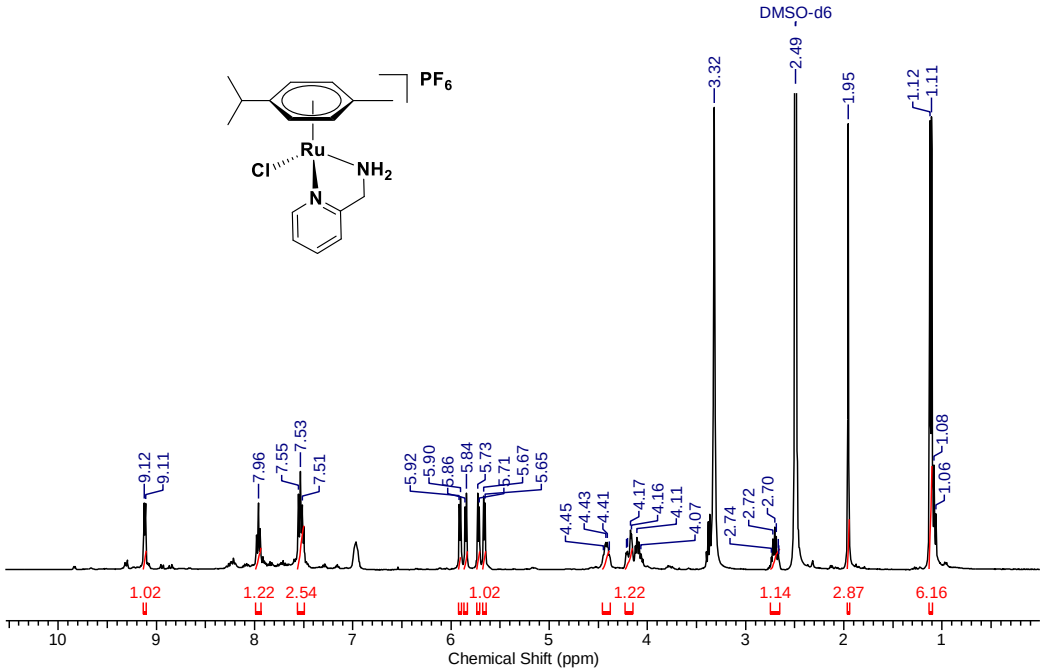

^{1}H NMR spectrum of **[Ru]-1** complex in DMSO-d_6

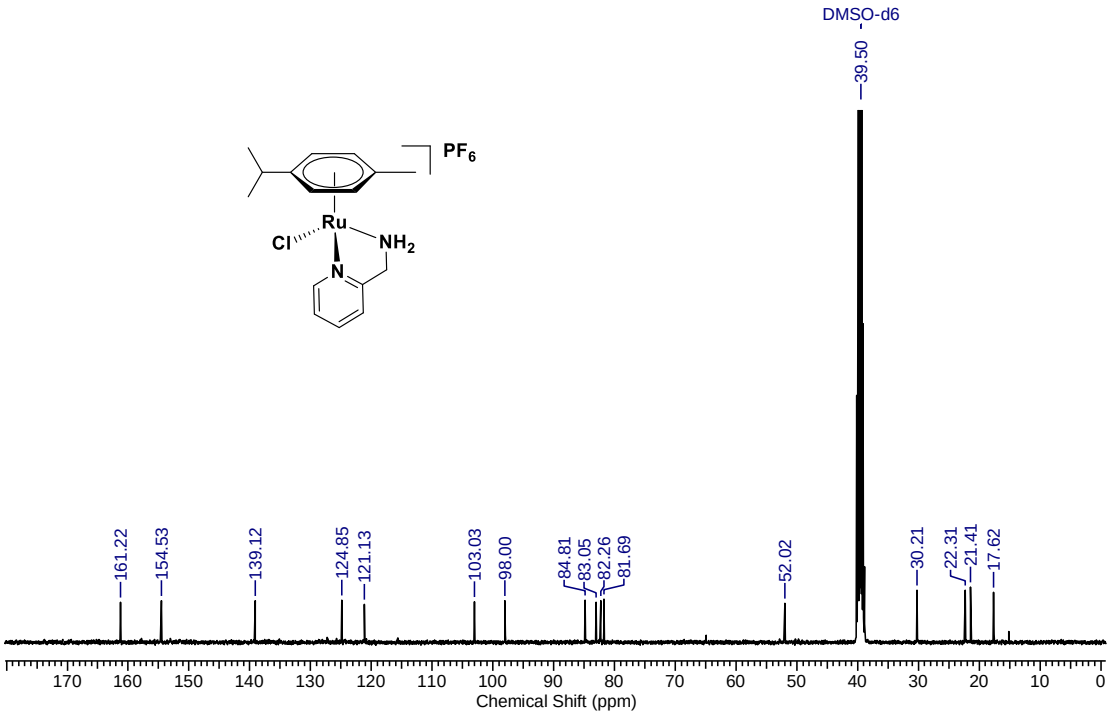

^{13}C NMR spectrum of **[Ru]-1** complex in DMSO-d_6

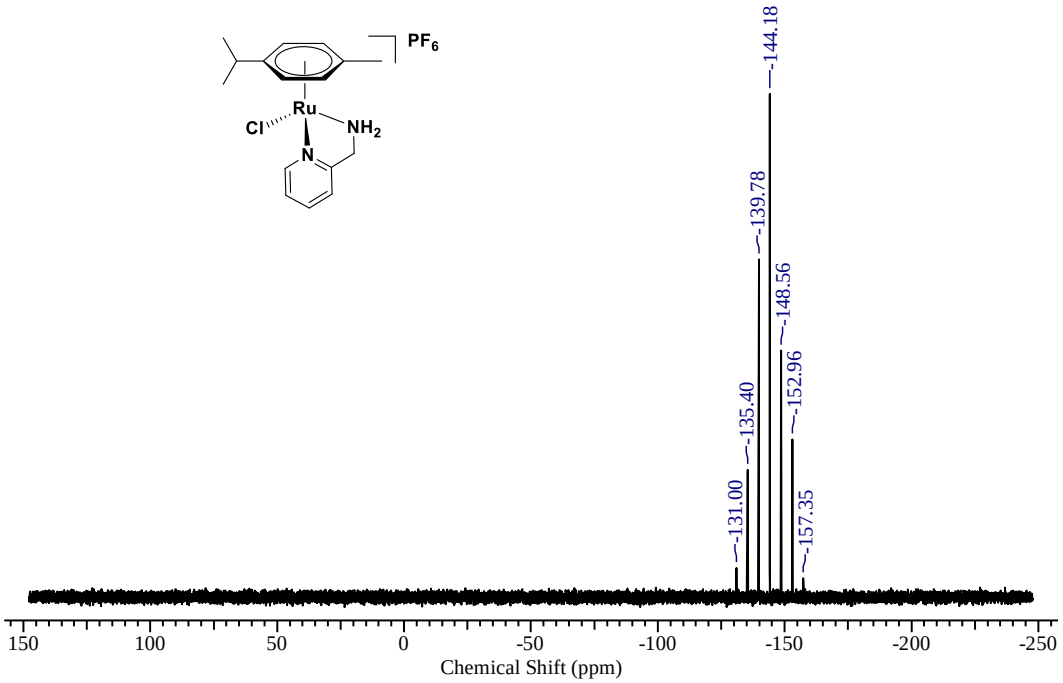

^{31}P NMR spectrum of **[Ru]-1** complex in DMSO-d_6

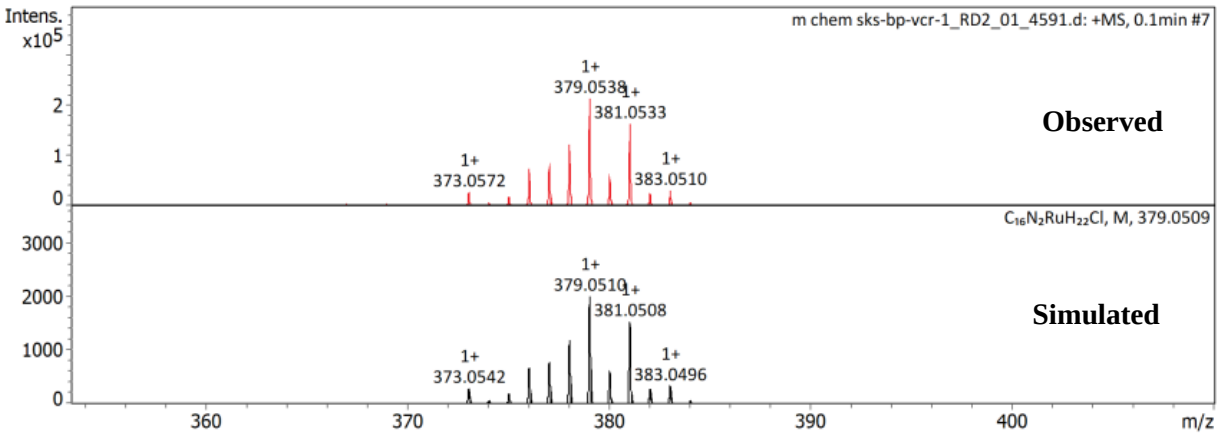

HR-MS of complex **[Ru]-1**

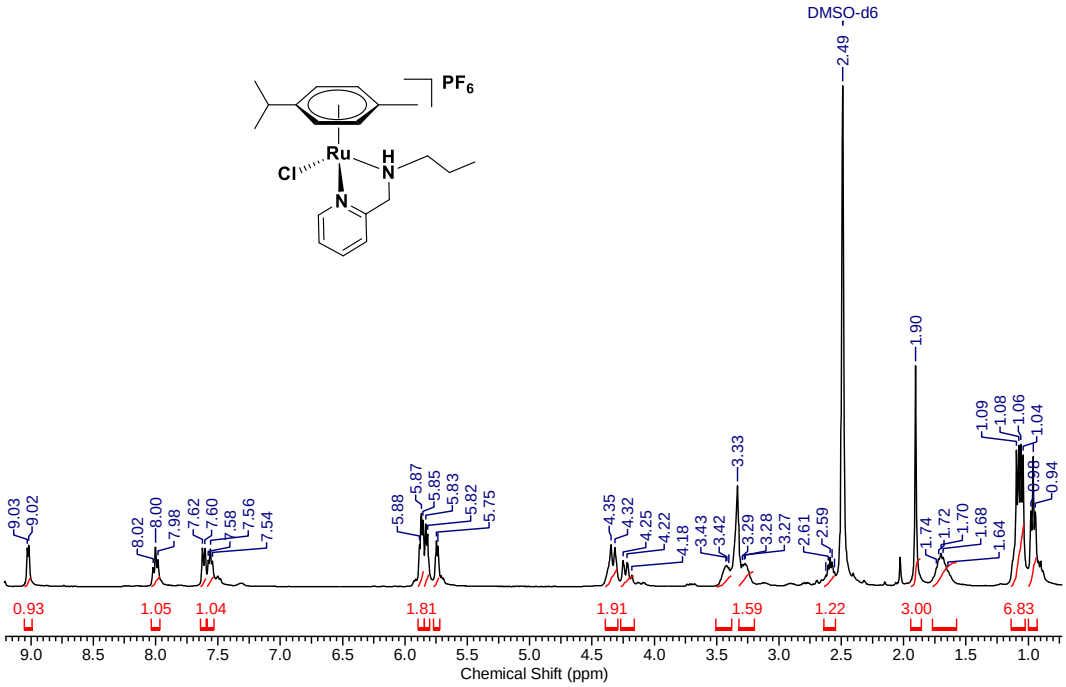

^{1}H NMR spectrum of **[Ru]-2** complex in DMSO-d_6

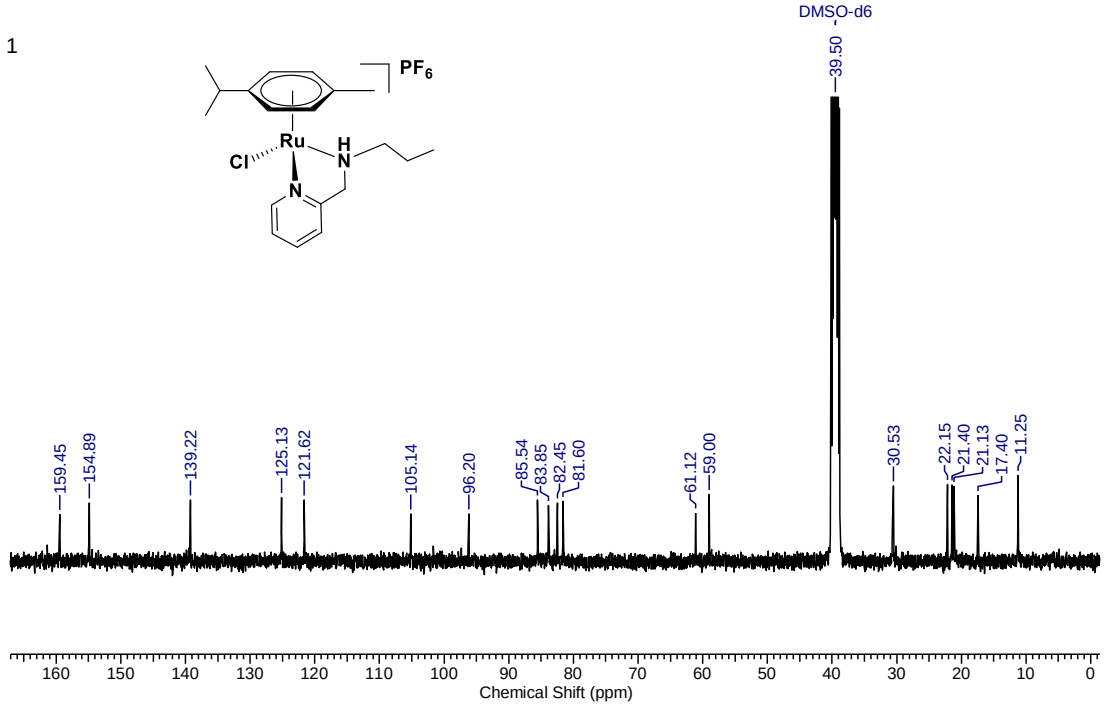

^{13}C NMR spectrum of **[Ru]-2** complex in DMSO-d_6

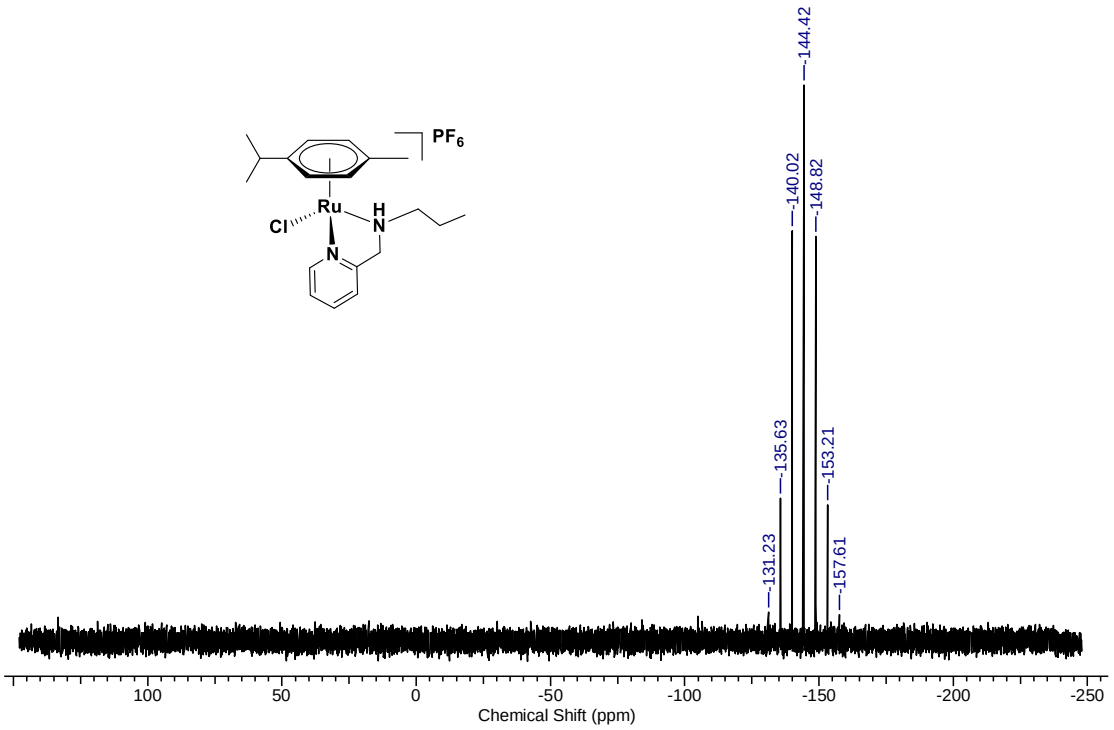

^{31}P NMR spectrum of **[Ru]-2** complex in DMSO-d_6

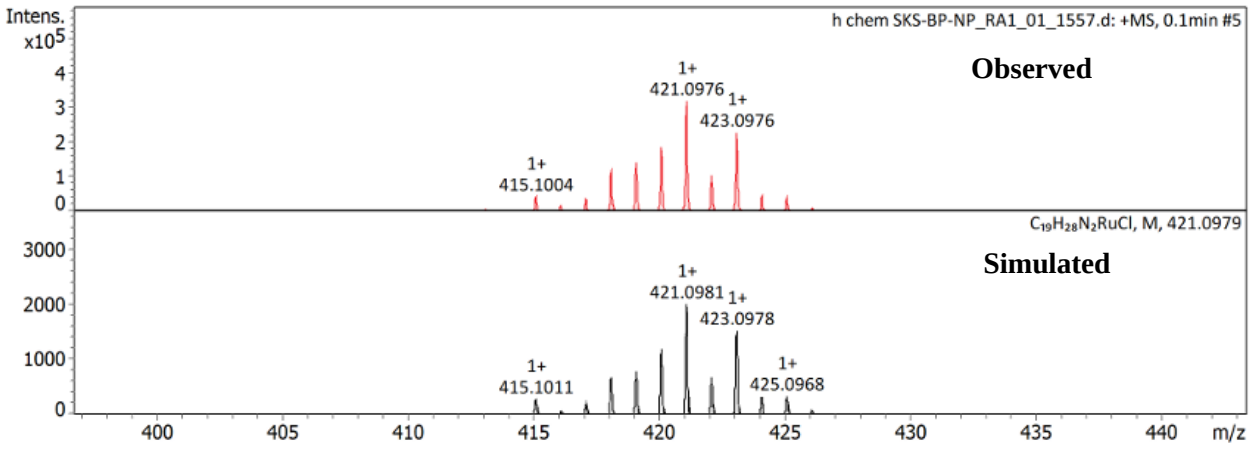

HR-MS of complex **[Ru]-2**

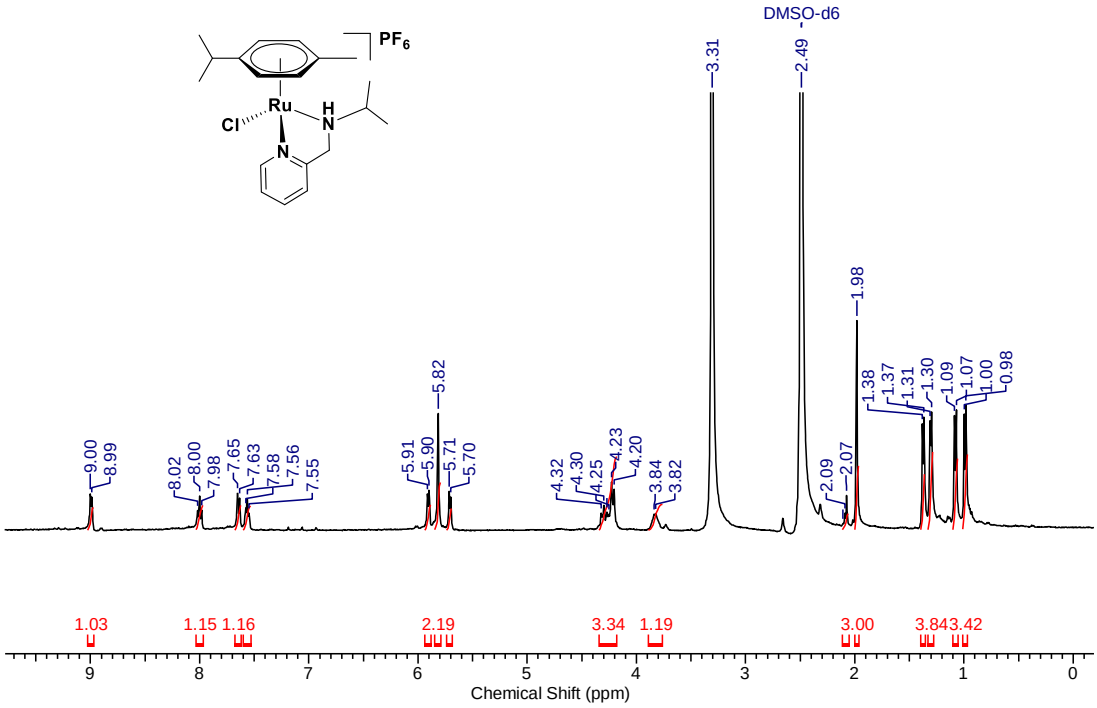

^{1}H NMR spectrum of [**Ru]-3** complex in DMSO-d_6

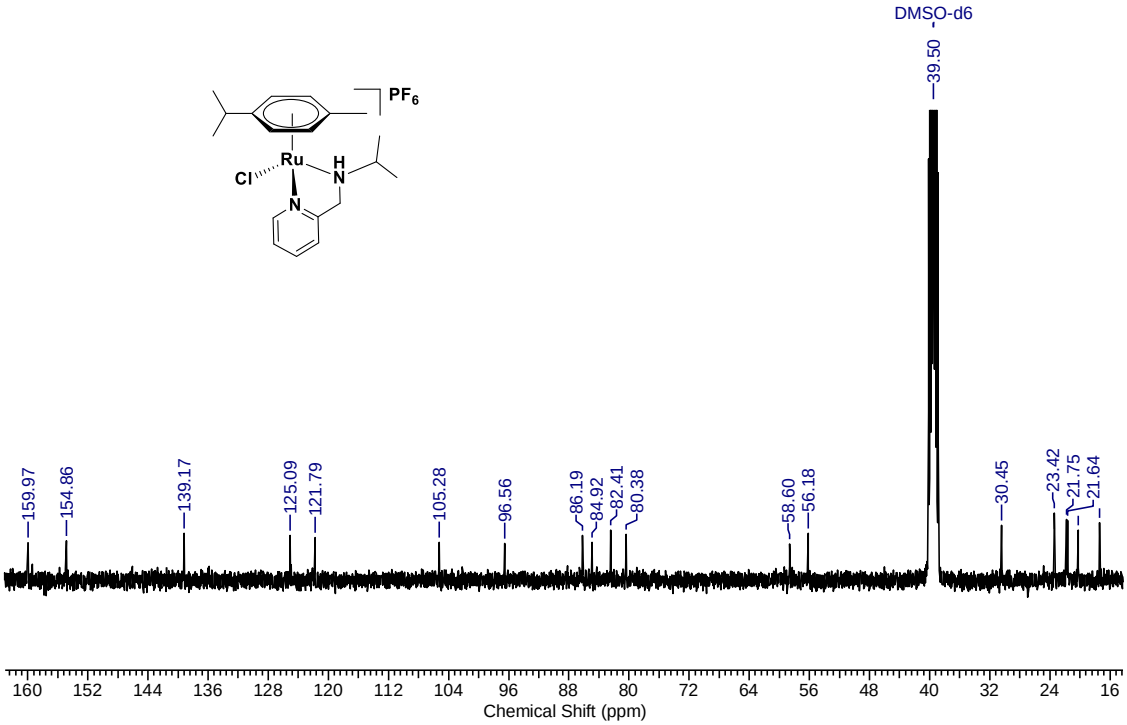

^{13}C NMR spectrum of [**Ru]-3** complex in DMSO-d_6

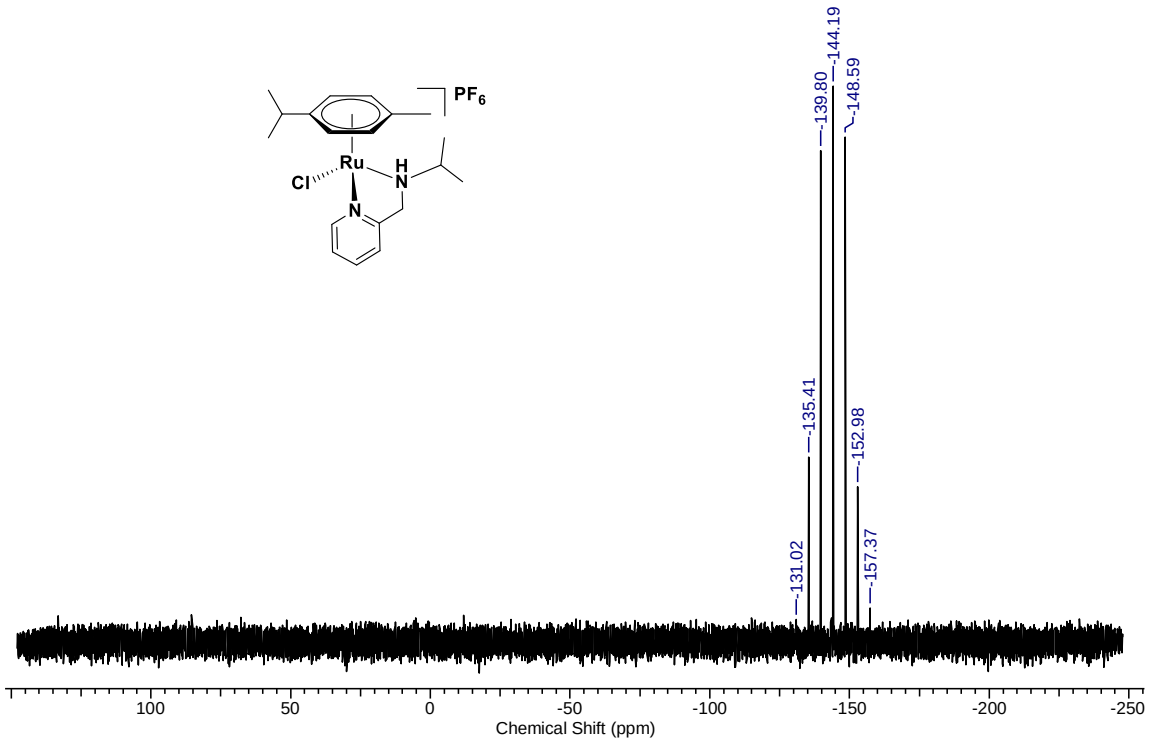

^{31}P NMR spectrum of **[Ru]-3** complex in DMSO-d_6

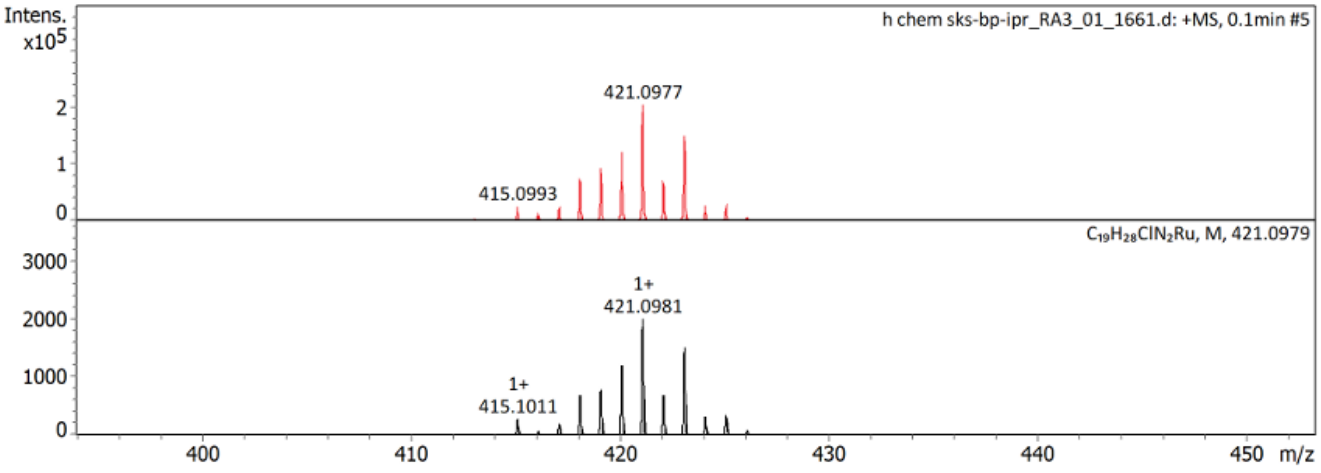

HR-MS of complex **[Ru]-3**

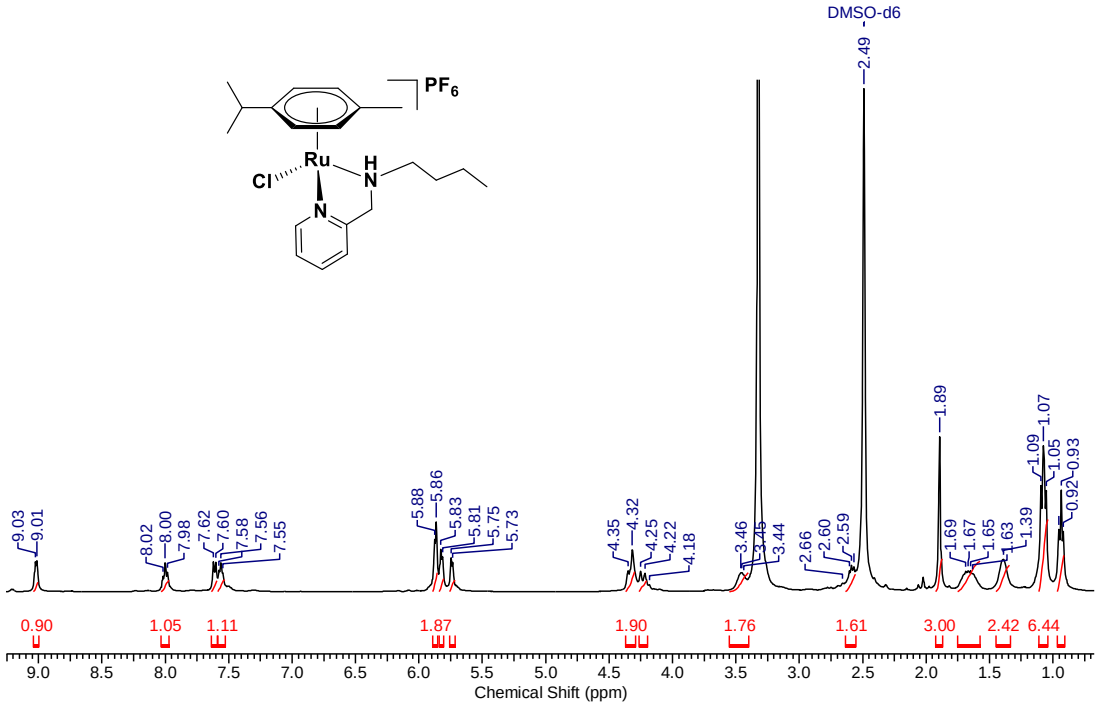

^{1}H NMR spectrum of **[Ru]-4** complex in DMSO-d_6

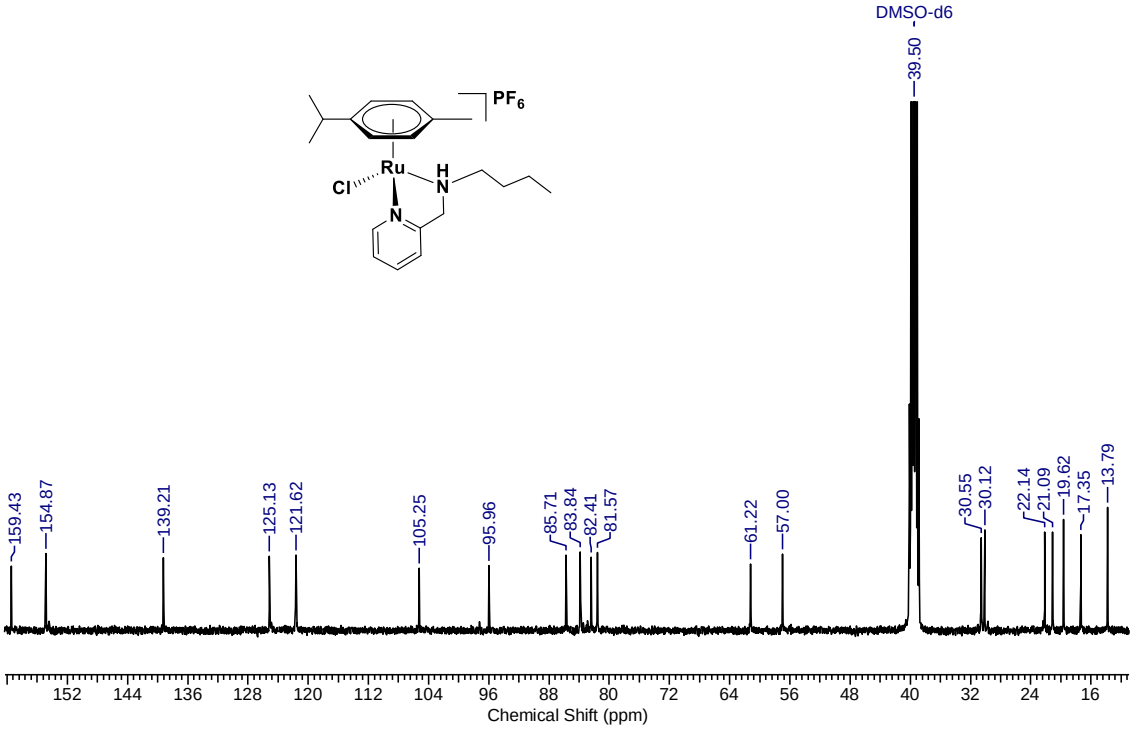

^{13}C NMR spectrum of **[Ru]-4** complex in DMSO-d_6

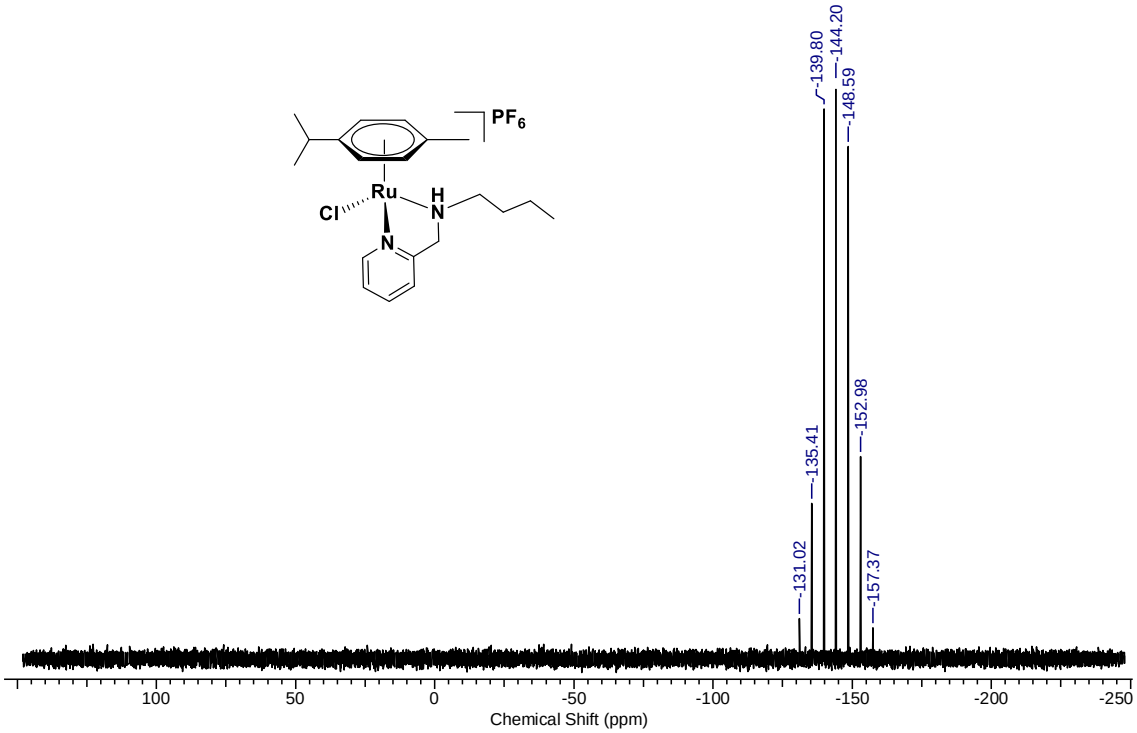

^{31}P NMR spectrum of **[Ru]-4** complex in DMSO-d_6

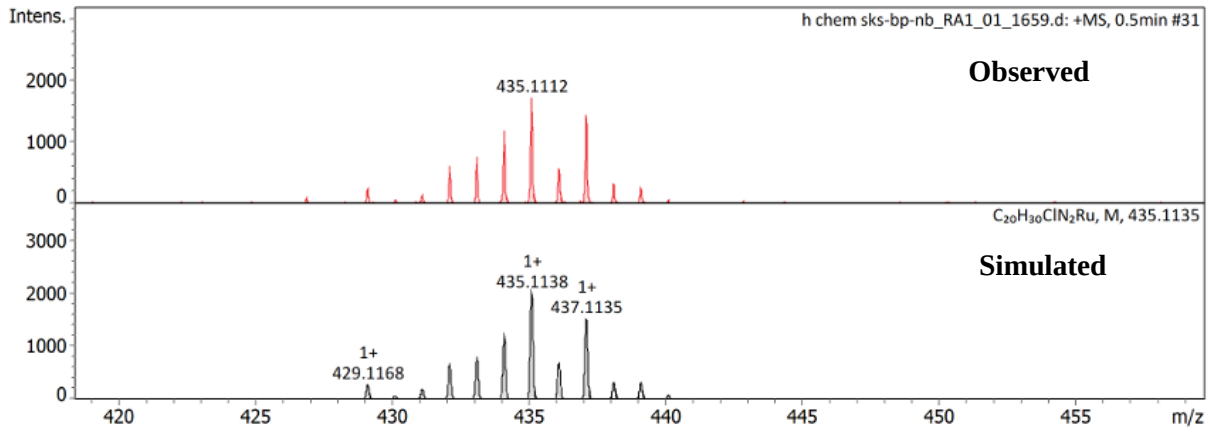

HR-MS of complex **[Ru]-4**

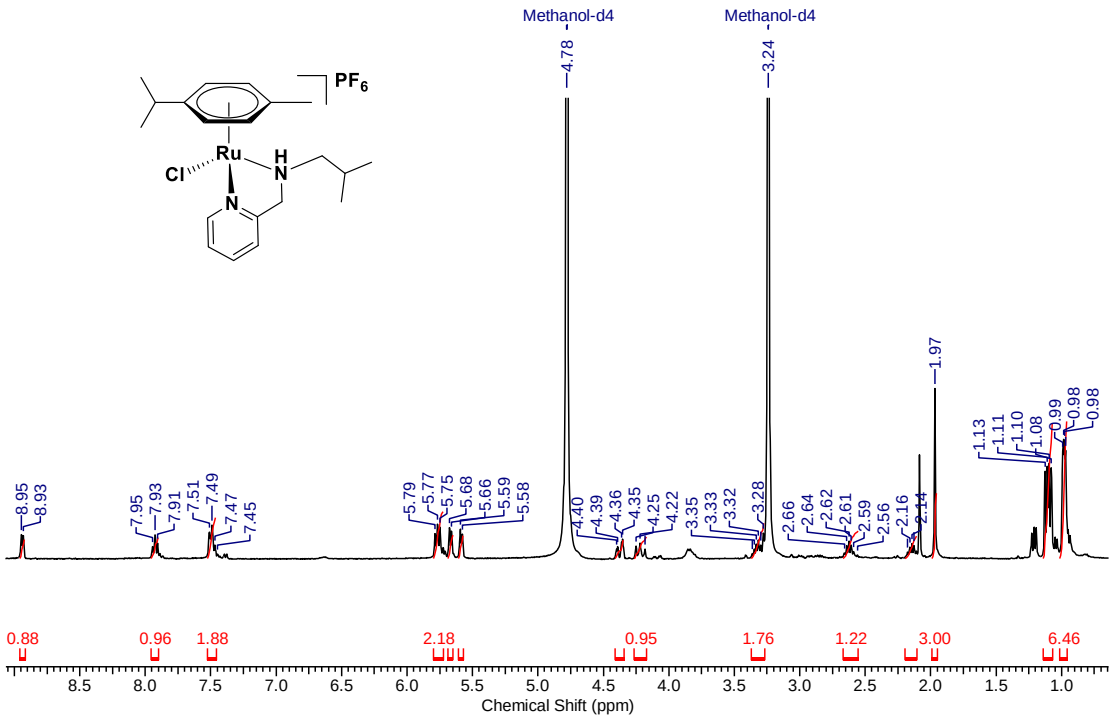

^{1}H NMR spectrum of **[Ru]-5** complex in methanol-d_4

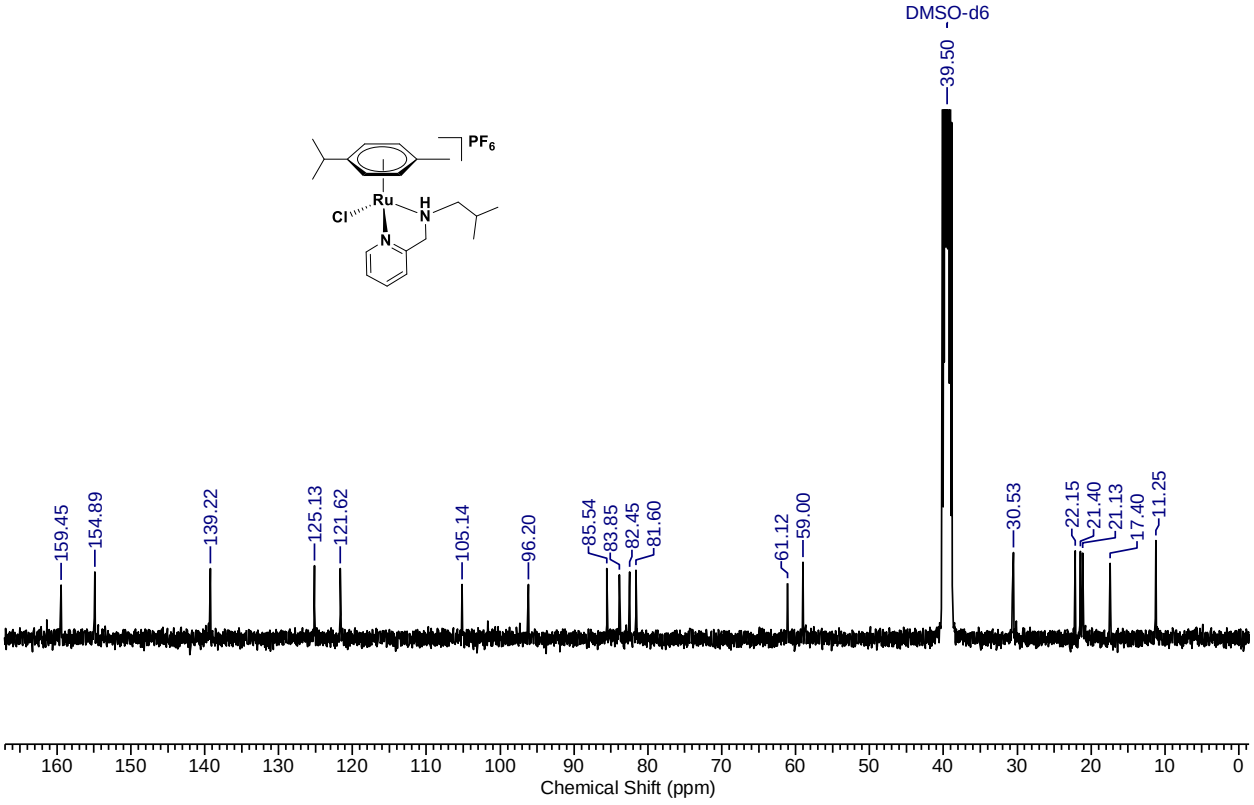

^{13}C NMR spectrum of **[Ru]-5** complex in dmso-d_6

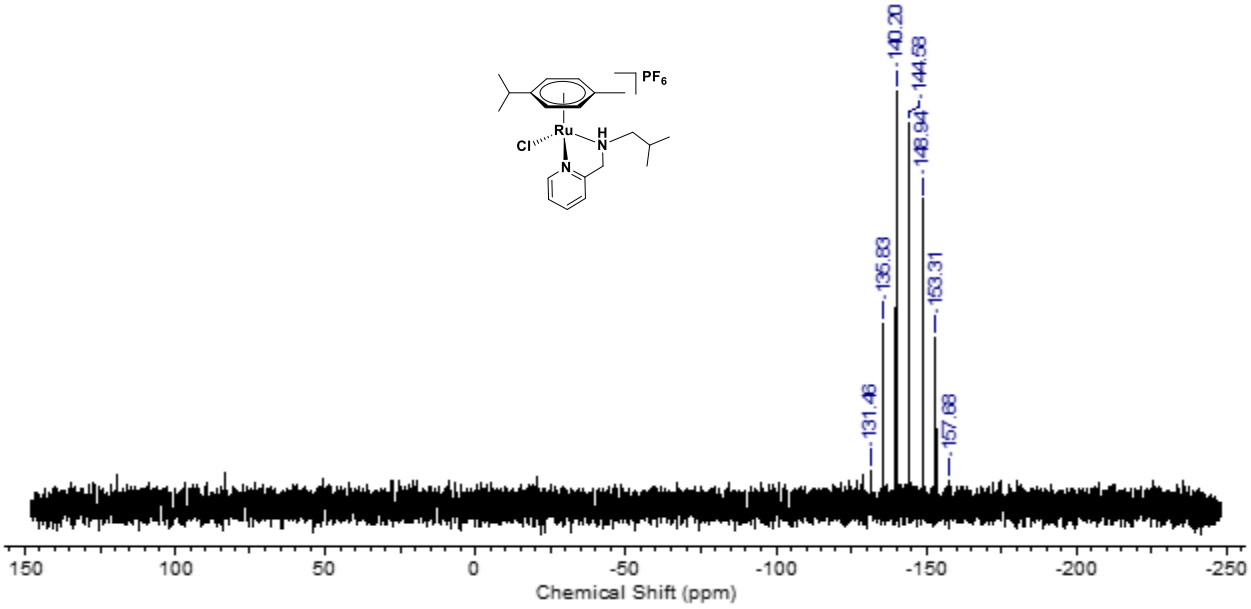

^{31}P NMR spectrum of **[Ru]-5** complex in methanol-d_4

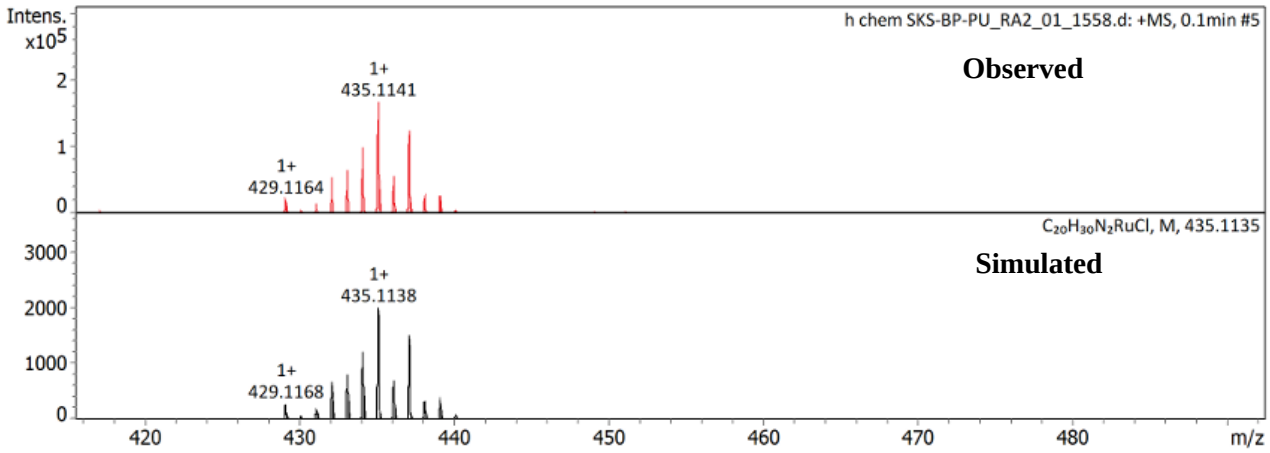

HR-MS of complex **[Ru]-5**

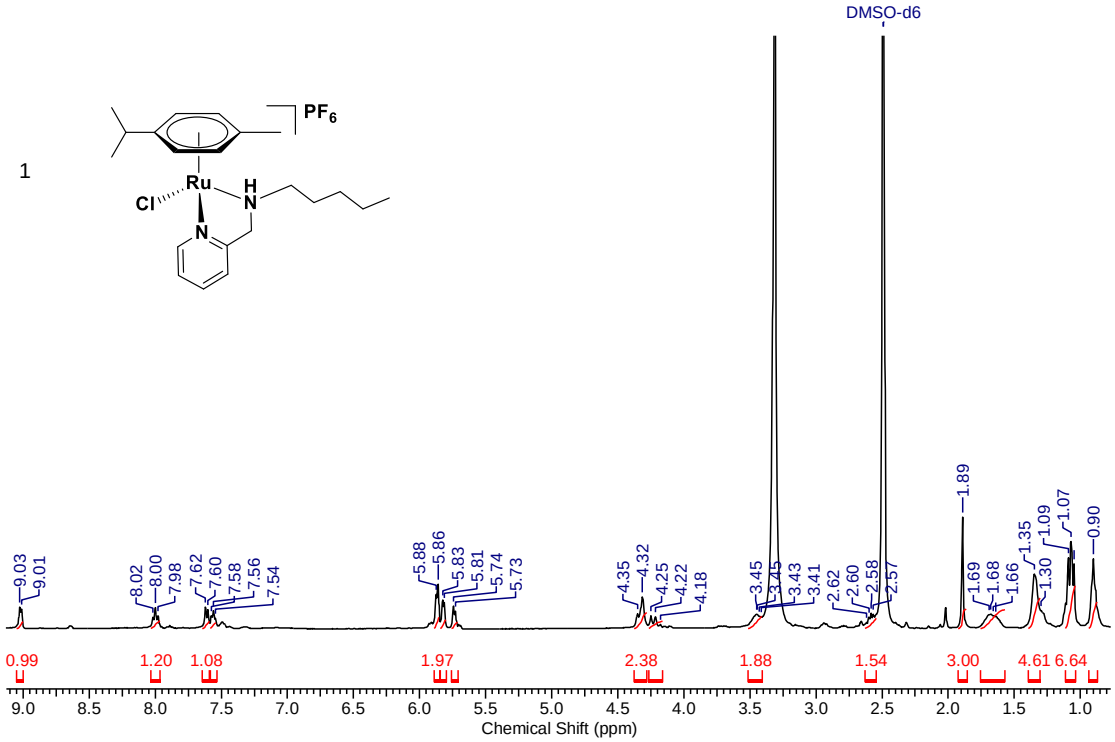

^{1}H NMR spectrum of **[Ru]-6** complex in DMSO-d_6

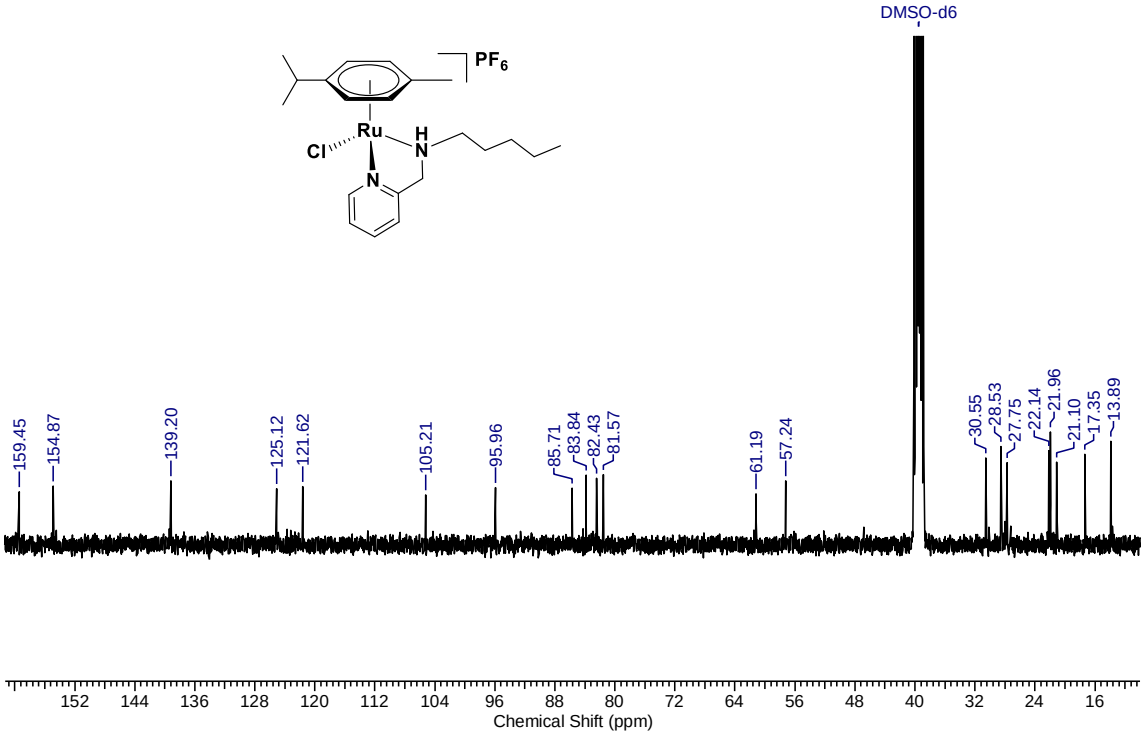

^{13}C NMR spectrum of [**Ru]-6** complex in DMSO-d_6

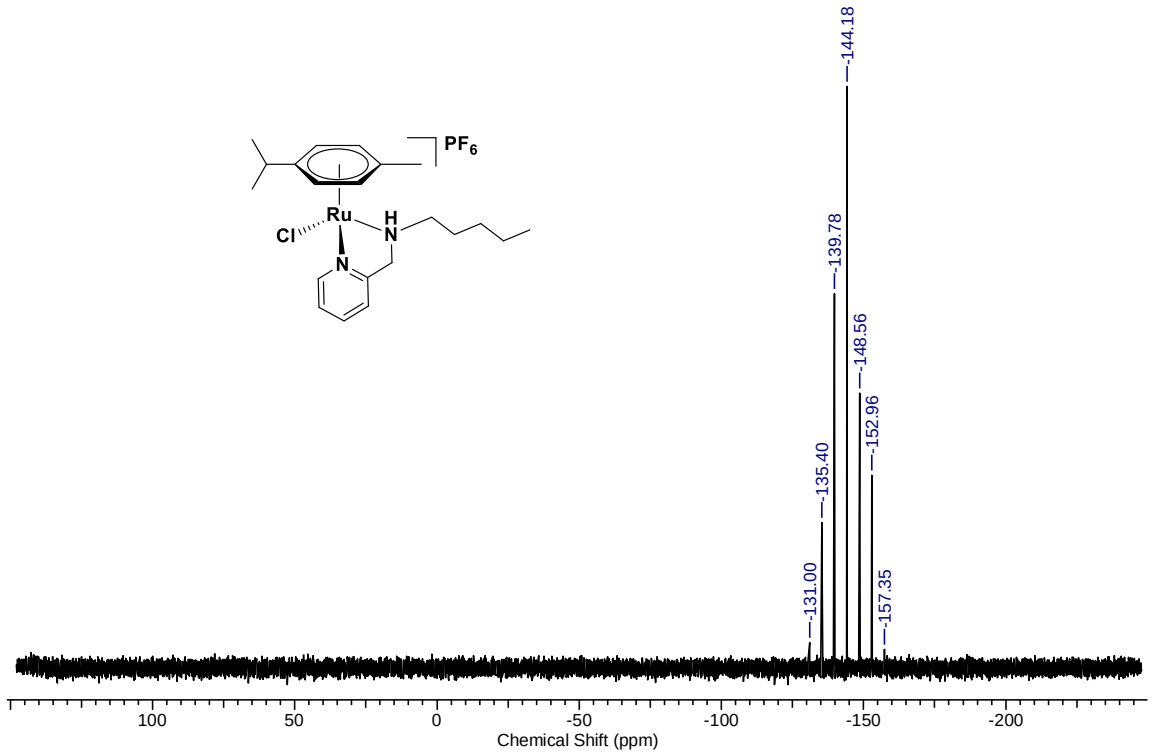

^{31}P NMR spectrum of **[Ru]-6** complex in DMSO-d_6

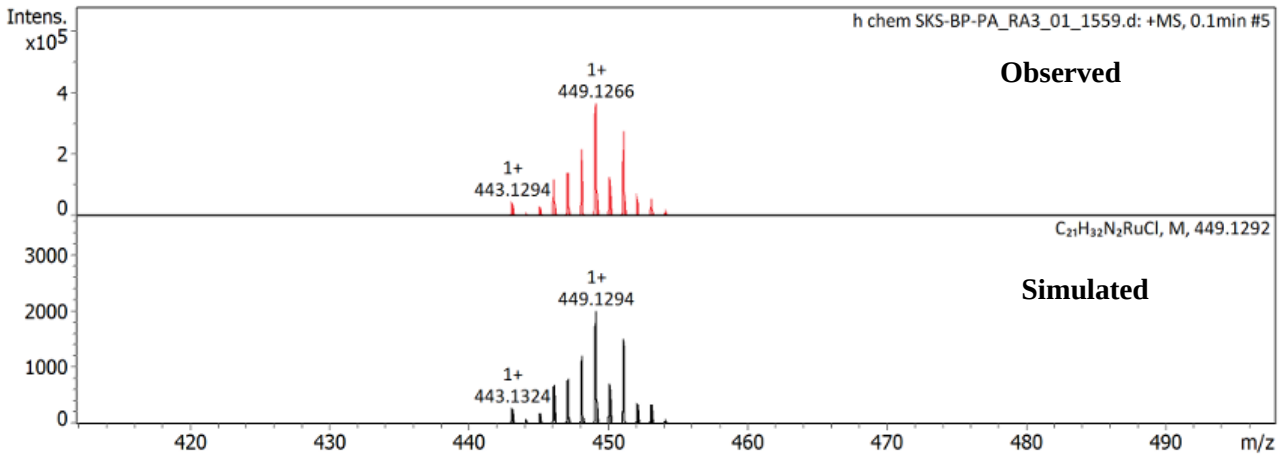

HR-MS of complex **[Ru]-6**

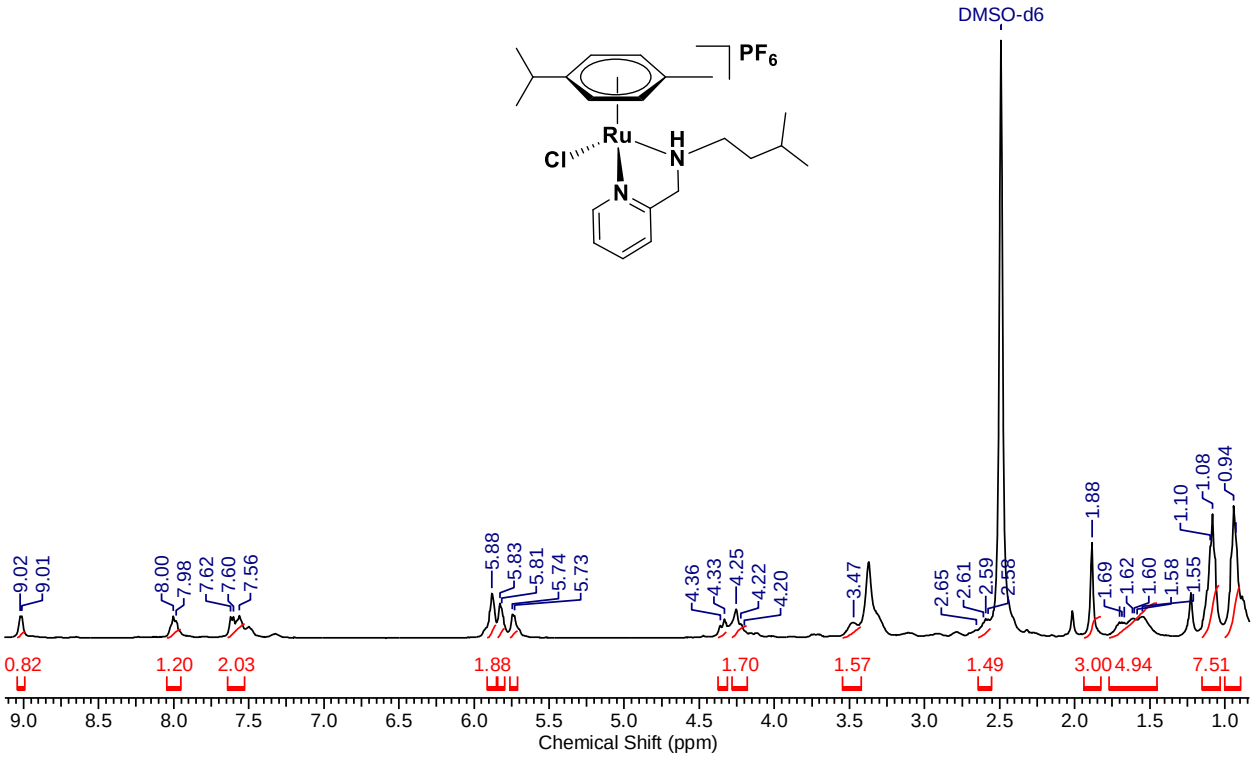

^{1}H NMR spectrum of **[Ru]-7** complex in DMSO-d_6

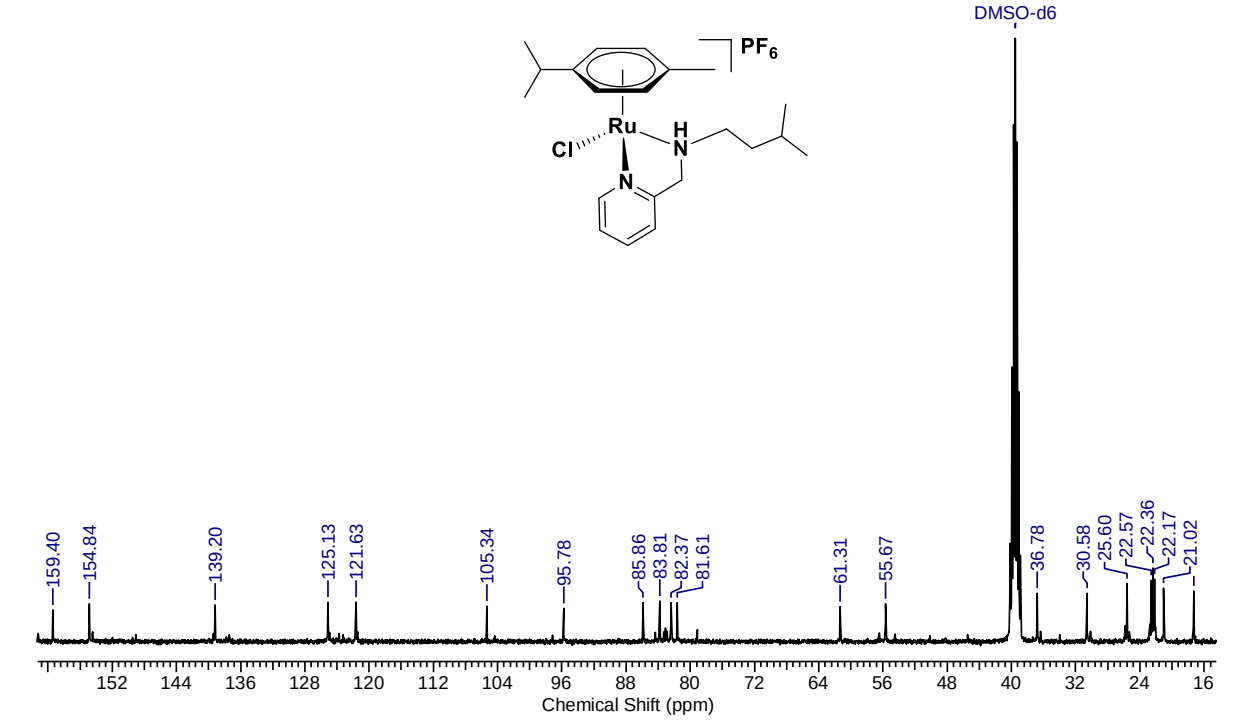

^{13}C NMR spectrum of [**Ru]-7** complex in DMSO-d_6

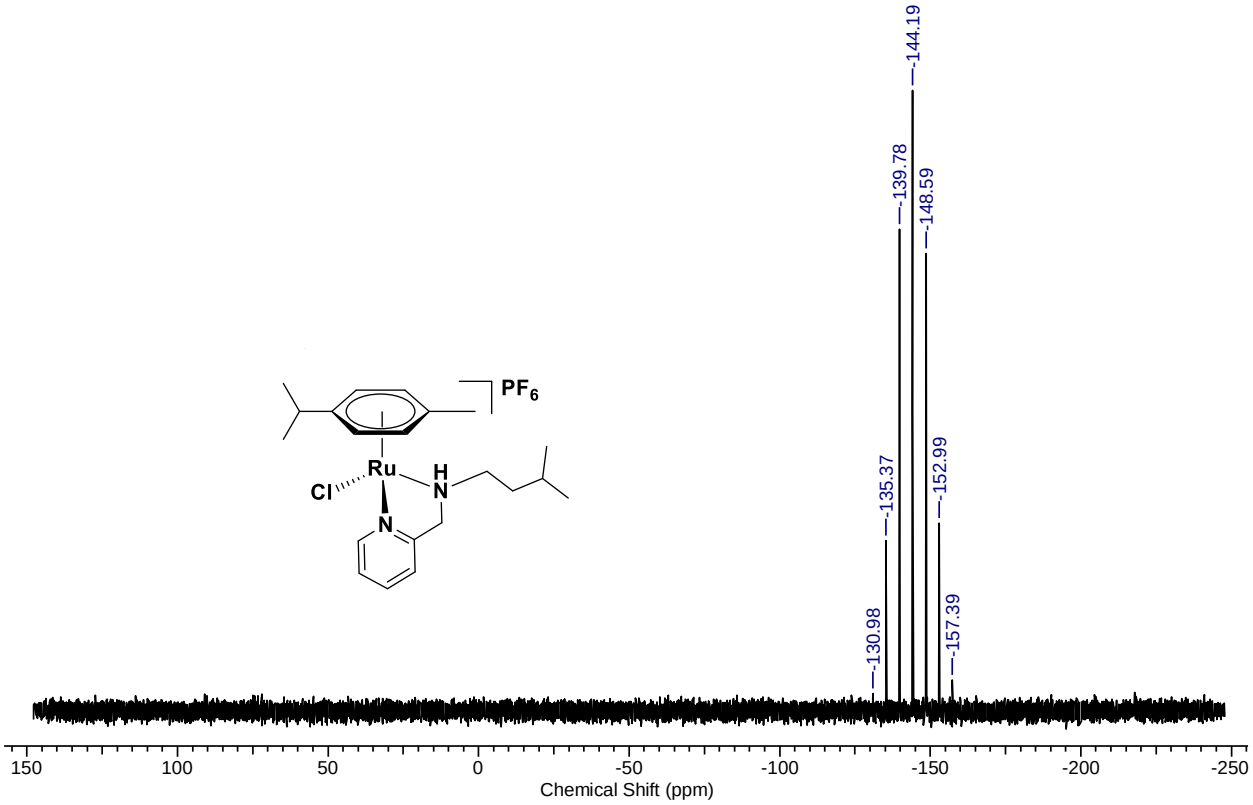

^{31}P NMR spectrum of **[Ru]-7** complex in DMSO-d_6

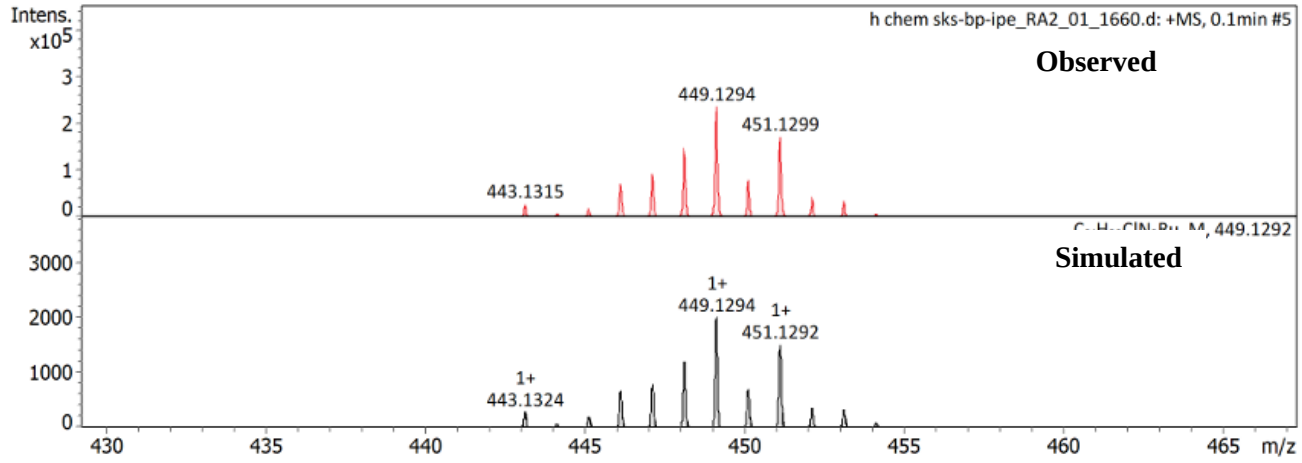

HR-MS of complex **[Ru]-7**

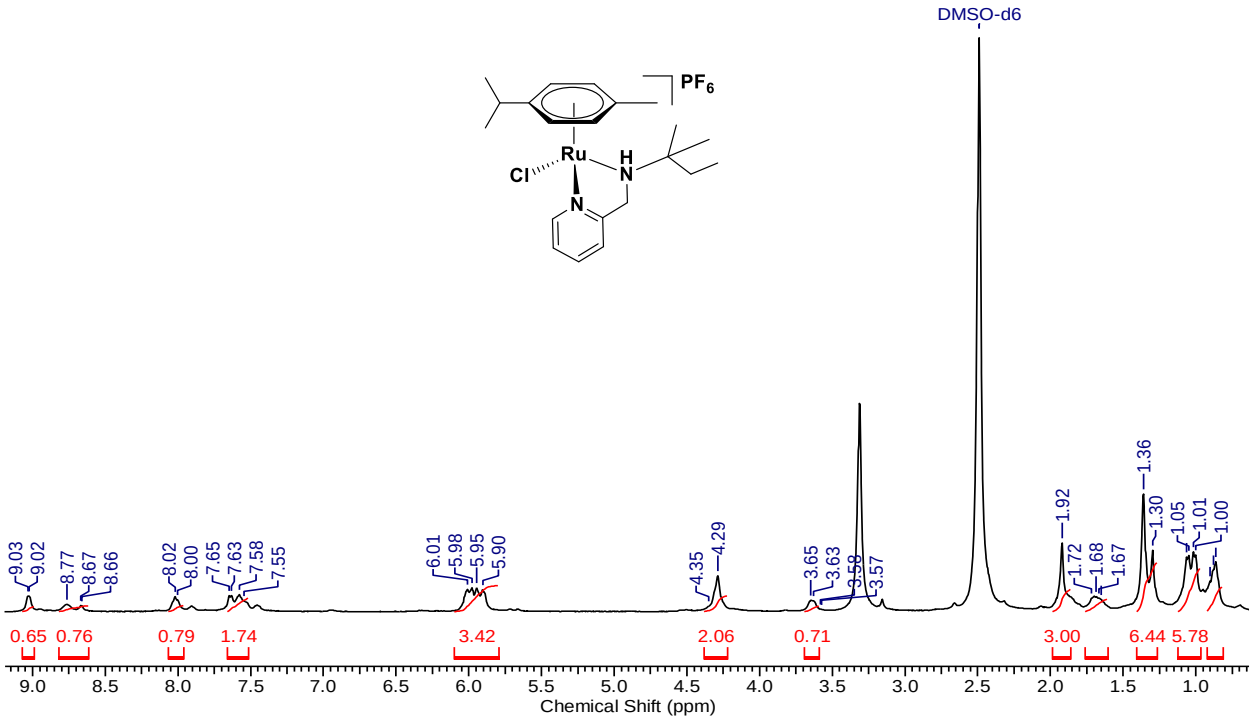

^{1}H NMR spectrum of **[Ru]-8** complex in DMSO-d_6

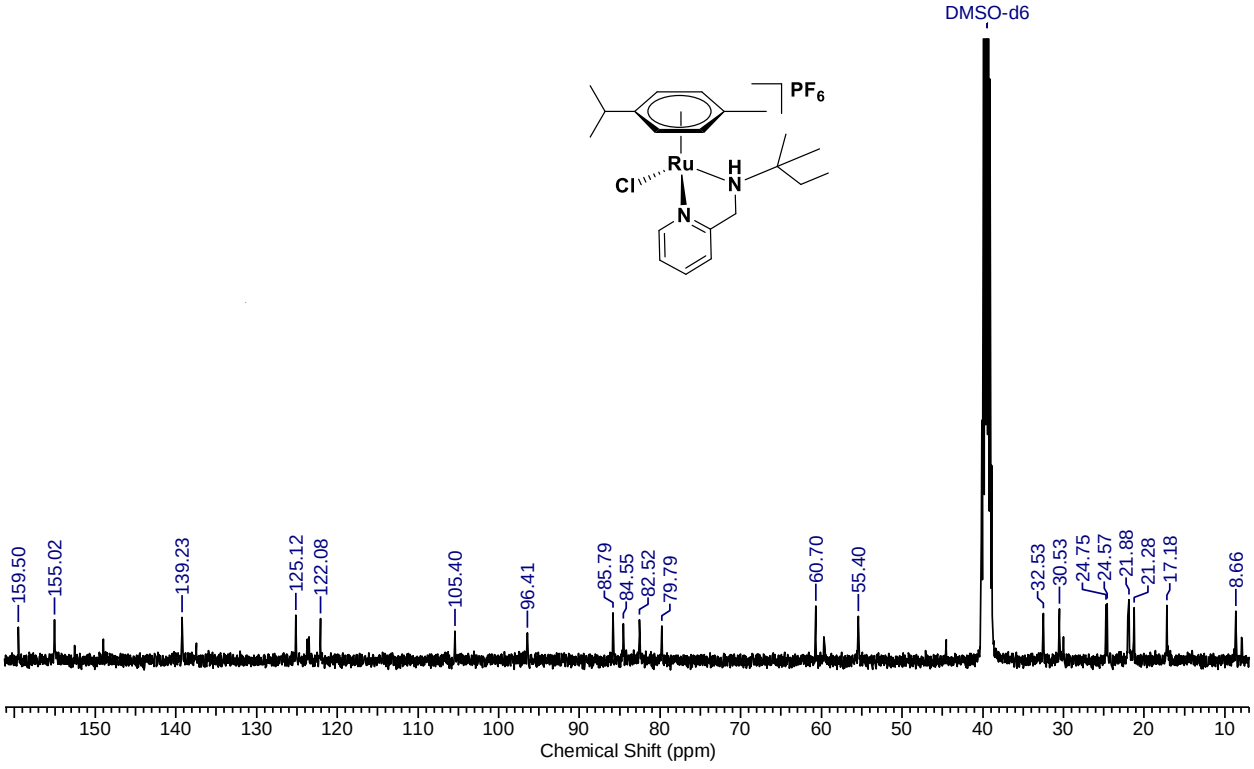

^{13}C NMR spectrum of **[Ru]-8** complex in DMSO-d_6

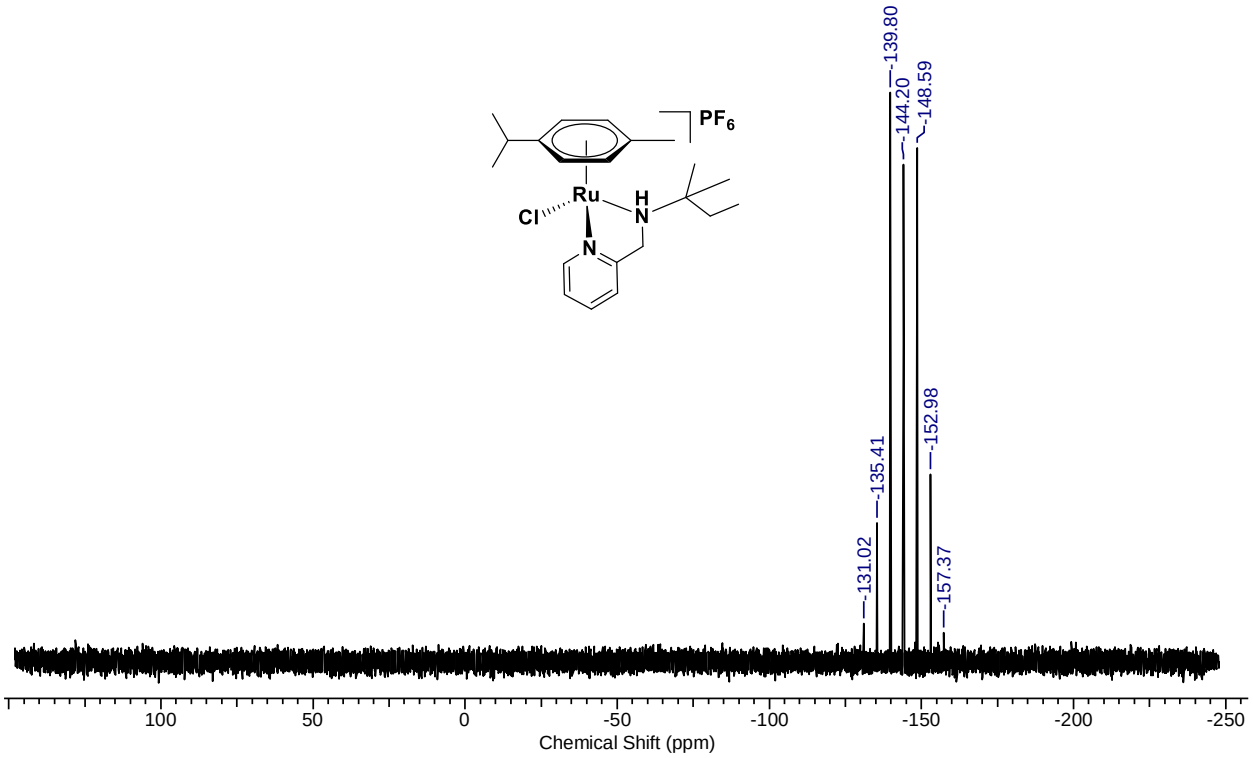

^{31}P NMR spectrum of **[Ru]-8** complex in DMSO-d_6

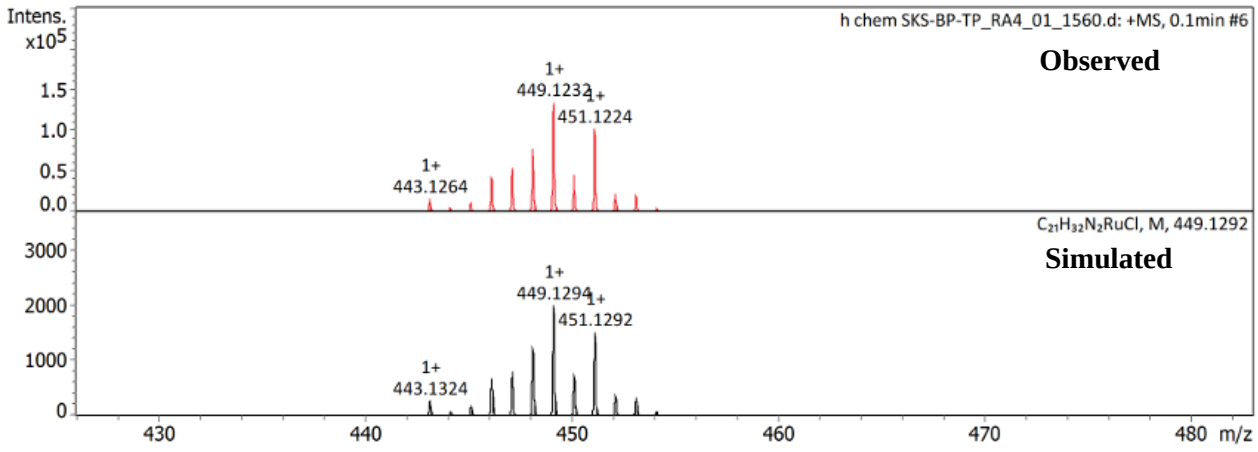

HR-MS of complex **[Ru]-8**

Spectral data of γ-valerolactone from levulinic acid:

γ-valerolactone (GVL): ^{1}H NMR (400 MHz, $CDCl_3$): δ (ppm) = 4.68-4.59 (m, 1H), 2.59-2.51 (t, 2H), 2.37-2.33 (m, 1H), 1.81-1.78 (m, 1H), 1.40-1.39 (d, 3H). ^{13}C NMR (100 MHz, $CDCl_3$): δ (ppm) = 177.28, 116.14, 29.70, 29.08, 21.08.

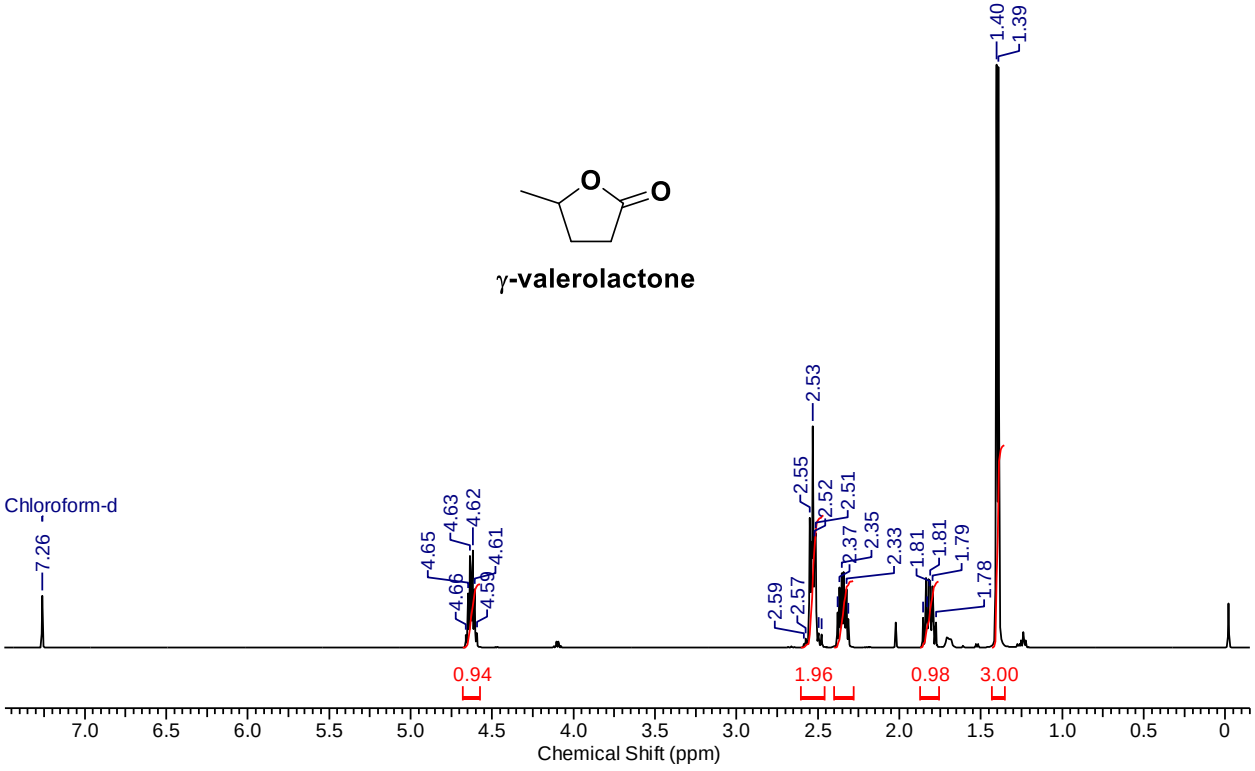

^{1}H NMR spectrum of γ-valerolactone

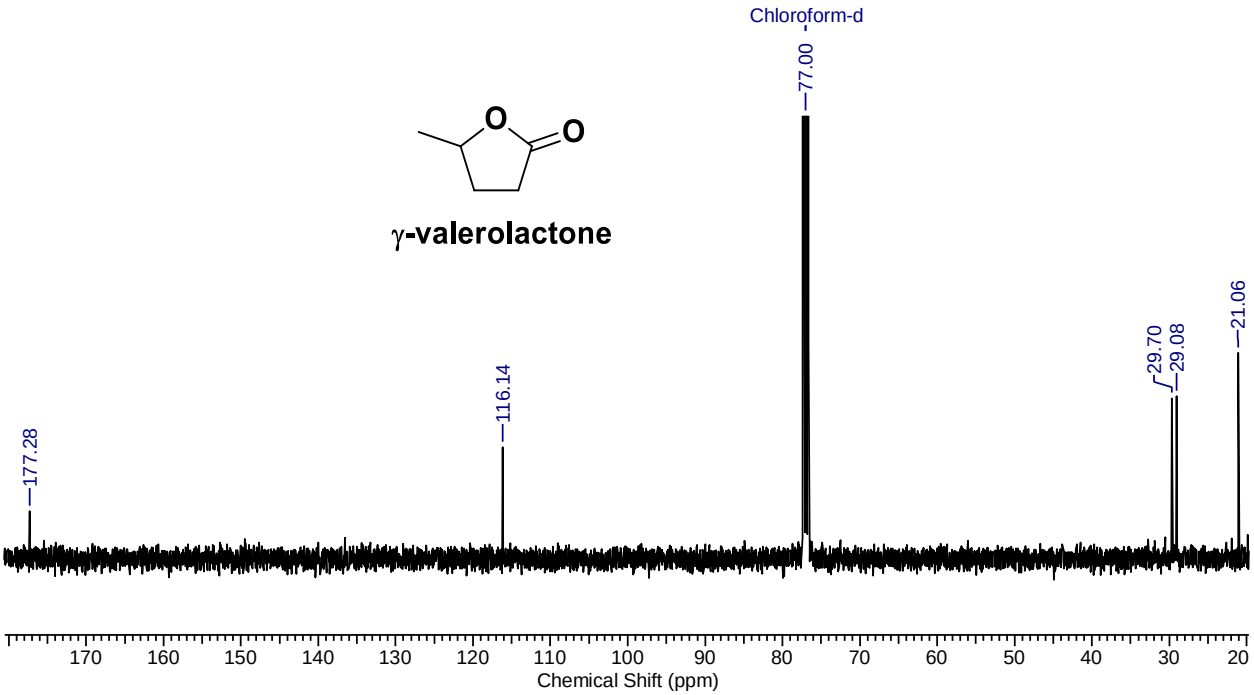

^{13}C NMR spectrum of γ-valerolactone

References

S1 H. Mehdi, V. Fabos, R. Tuba, A. Bodor, L.T. Mika, I. T. Horvath, *Top. Catal.*, 2008, **48**, 49–54.

S2 J. Deng, Y. Wang, T. Pan, Q. Xu, Q.-X. Guo, Y. Fu, *ChemSusChem*, 2013, **6**, 1163-1167.

S3 A. D. Chowdhury, R. Jackstell, M. Beller, *ChemCatChem*, 2014, **6**, 3360–3365.

S4 J. M. Tukacs, D. Kiraly, A. Stradi, G. Novodarszki, Z. Eke, G. Dibo, T. Kegl, L. T. Mika, *Green Chem.*, 2012, **14**, 2057–2059.

S5 F. M. A. Geilen, B. Engendahl, M. Holscher, J. Klankermayer, W. Leitner, *J. Am. Chem. Soc.*, 2011, **133**, 14349–14358.

S6 V. Fabos, L. T. Mika, I. T. Horvath, *Organometallics*, 2014, **33**, 181–187.

S7 G. Amenuvor, B. C. E. Makhubela, J. Darkwa, *ACS Sustainable Chem. Eng.*, 2016, **4**, 6010−6018.

S8 N. K. Oklu, B. C. E. Makhubela, *Inorg. Chimica Acta*, 2018, **482**, 460-468.

S9 U. Omoruyi, S. J. Page, S. L. Apps, A. J. P. White, N. J. Long, P. W. Miller, *J. Organomet. Chem.*, **2021**, 935, 121650-121662.

S10 G. Amenuvor, C. K. Rono, J. Darkwa, B. C. E. Makhubela, *Eur. J. Inorg. Chem.*, 2019, ***36***, 3942-3953.

S11 C. A. M. R. Slagmaat, M. A. F. Delgove, J. Stouten, L. Morick, Y. Meer, K. V. Bernaerts, S. M. A. D. Wildeman, *Green Chem.*, 2020, ***22***, 2443-2458.

S12 A. D. Dwivedi, V. K. Sahu, S. M. Mobin, S. K. Singh, *Inorg. Chem.*, 2018, **57**, 4777–4787.

S13 Y. -C. Lin, K. -H. Yu, S. -L. Huang, Y. -H. Liu, Y. Wang, S. -T. Liu, J. -T. Chen, *Dalton Trans*., 2009, 9058-9067.

S14 M. Carmona, R. Rodriguez, I. Mendez, V. Passarelli, F. J. Lahoz, P. Garcia-Orduna, D. Carmona, *Dalton Trans.*, 2017, **46**, 7332-7350.

S15 P. Govindaswamy, Y. A. Mozharivskyj, M. R. Kollipara, *Polyhedron*, 2004, **23**, 1567-1572.

S16 M. K. Awasthi, S. K. Singh, *Inorg. Chem.*, 2019, **58**, 14912–14923.